MASTERARBEIT | MASTER'S THESIS

Titel | Title

Dam Good Deposits: Unravelling Secrets of a Dammed Lake in Salzburg's Quaternary Record

A Sedimentological Study on Fluvial, Deltaic, Lacustrine and Glacial Sediments and Landforms prior to the Last Glacial Maximum in Embach

verfasst von | submitted by

Lukas Eder BSc

angestrebter akademischer Grad | in partial fulfilment of the requirements for the degree of

Master of Science (MSc)

Wien | Vienna, 2025

Studienkennzahl lt. Studienblatt | Degree programme code as it appears on the student record sheet:	UA 066 815
Studienrichtung lt. Studienblatt | Degree programme as it appears on the student record sheet:	Masterstudium Erdwissenschaften
Betreut von | Supervisor:	Univ.-Prof. Daniel Le Heron PhD

Acknowledgments

This work would not have been possible on my own. It is the result of collaboration between many wonderful people, and I am infinitely grateful to each and every one of them. I would like to dedicate this work to these people and take this opportunity to express my deepest gratitude and sincere appreciation to them.

To my supervisor, Prof. Daniel Le Heron, Dan: the time working with you means a lot to me. Thank you for your constant support, your way of mentoring and teaching, your expertise, your understanding and patience. And thank you for standing in the pouring rain and still laughing at my corny jokes.

I also want to thank the International Association of Sedimentologists, IAS, for granting this project with the Judith McKenzie Fieldwork Award and to University of Vienna, which also funded the project. Without this financial support, fieldwork would not have been feasible.

In keeping with the theme, I would like to express my sincere thanks to Michael Nagl, who accompanied me in the field in the most adverse conditions and provided me with tremendous support. Thank you for freezing our ar**s off together and making weird green hot water.

Furthermore, I would like to deeply thank Prof. Susanne Gier for her help while doing lab work, XRD analysis and always helping with related problems and questions. I would also like to thank Ricarda Wohlschlägl und Paulina Mejias-Osorio, for having important feedback and your help during analysis.

To my colleagues, thank you for making this time at university so special. I will certainly not forget it, especially one or two stories about the excursions…

I would also like to express my sincere gratitude to my parents. Without your support, my studies would not have been possible.

And last but not least, I would like to express my deepest gratitude to my partner Susi. Thank you for always being there, listening, giving advice and feedback and supporting me, despite your own stress. I see that and I really appreciate it all the more. Your shire-like character could always calm my nervous system (despite the axe embedded in my skull) and your laughter lifted me out of even the deepest trough valleys.

Thanks again to everyone with whom I was able to walk this path. Hopefully we will continue to stumble along together for a long time to come!

To conclude by quoting Tolkien: "His old life lay behind the mists, dark adventure lay in front…".

Oder, um es mit den Worten des großen Dr. Michael Häupl zu sagen:

MAN BRINGE DEN SPRITZWEIN!

Acknowledgment of AI usage

I hereby acknowledge the usage of the AI tools perplexity (https://www.perplexity.ai/) and deepl (https://www.deepl.com/de/translator) to help me in the refinement of my academic language and to generally identify improvements in the writing style and spelling. I confirm that I have read and understood the AI usage guidelines from the UNIVIE and that this thesis complies with them.

Abstract

The Quaternary record of Austria preserves a rich archive of glacial and paraglacial deposits, including thick successions in major trough valleys. At Embach, 60 km southwest of Salzburg in the Salzach Valley, an at least 80 m thick succession of gravels and sands is exposed and capped by a till deposited by the Salzach trunk glacier at the Last Glacial Maximum (LGM). The village of Embach is situated directly above this succession, which forms part of an active mass movement and thus substantial stabilisation efforts were made since the 20th century. Despite this, the origin of the sands and gravels, and the associated landscape evolution during the last interglacial (Marine Isotope Stage 5e), have remained poorly constrained. Here, integrated analysis of UAV-based photogrammetry, high-resolution (1 m) laser-scan topography, field profiling and mapping, X-ray diffraction, granulometry and clast fabric demonstrates that the Embach succession records a mixed delta–fluvial system developed in a partly lake-filled Salzach Valley prior to the LGM. Large-scale foreset beds indicate delta deposition, whereas imbricated, channelised and sheet gravels record persistent fluvial activity. Within a sequence-stratigraphic framework, several lake-level rise–fall cycles are recognised, and measured palaeoflow indicators (foresets, imbrications, drumlins) show north- and east-directed flow into the Salzach Valley. The results imply that earlier interpretations of the *Deckenschotter* as purely fluvial deposits require revision. A range of mechanisms is proposed for lake formation and relative lake-level fluctuations, including mass movements and the collapse or reorganisation of lateral moraines and alluvial fans, enabling a detailed palaeoenvironmental reconstruction. These findings extend recent Quaternary sedimentological and geomorphological work in Austrian trough valleys and have direct relevance for hazard assessment in populated areas underlain by Quaternary deposits. For Embach in particular, a robust understanding of sedimentary architecture and Quaternary history is crucial for designing future mitigation measures on the active mass movement.

Kurzfassung

In der Gemeinde Embach, 60 km südwestlich von Salzburg im Salzachtal gelegen, ist eine mindestens 80 m mächtige Abfolge von Kies und Sand aufgeschlossen, teils von Till bedeckt. Dieser wurde vom Salzachgletscher während des letzten glazialen Maximums (LGM) abgelagert. Das Dorf Embach liegt direkt oberhalb dieser Abfolge, welche Teil einer aktiven Massenbewegung ist, weshalb seit dem 20. Jahrhundert erhebliche Stabilisierungsmaßnahmen durchgeführt wurden. Dennoch sind die Herkunft der Sande und Kiese und die damit verbundene Landschaftsentwicklung während der letzten Warmzeit (Marine Isotope Stage 5e) kaum erforscht. Anhand einer Analyse von hochauflösenden 3D Modellen, hochauflösenden (1 m) Laserscans, Sedimentprofilen und Geomorphologischen Karten, Röntgendiffraktogrammen (XRD) und Kornsummenkurven, zeigt diese Arbeit, dass die sedimentäre Abfolge in Embach ein Fluss-, beziehungsweise Deltasystem dokumentiert, welches sich vor dem LGM in einem See im Salzachtal entwickelt hat. Großmaßstäbige Foresets weisen auf Ablagerung in einem Delta hin, Imbrikationen und Fließkanalstrukturen dokumentieren fluviatile Bedingungen. Durch Sequenzstratigraphie (Wheeler-Diagramm) wurden mehrere Transgressions- und Regressionszyklen des relativen Seespiegels erkannt. Foresets, Imbrikationen und Drumlins zeigen eine nach Norden und Osten, in das Salzachtal gerichtete Fließrichtung. Die Ergebnisse implizieren, dass frühere Interpretationen der *Deckenschotter* als rein fluviatile Ablagerungen einer Revision bedürfen. Mehrere Mechanismen werden für die Entstehung des Sees vorgeschlagen, unter anderem Massenbewegungen, Kollabieren von Seitenmoränen oder Schwemmfächer. Diese Arbeit ergänzt die neuesten sedimentologischen und geomorphologischen Arbeiten zum Quartär in österreichischen Trogtälern und ist von großer Relevanz für die Bewertung von geogenen Naturgefahren in besiedelten Gebieten mit quartärem Untergrund. Insbesondere für Embach ist ein fundiertes Verständnis der sedimentären Architektur und der quartären Geschichte von entscheidender Bedeutung für die Planung zukünftiger Maßnahmen bezüglich der Massenbewegung.

Table of contents

1 Introduction

1.1 Preamble

The Embach section in the Salzach Valley, Austria, exposes an ~80 m thick pre-Last Glacial Maximum (LGM) succession of sands and gravels capped by till, offering a rare window into interglacial landscape evolution in an overdeepened Alpine trough valley prone to modern mass movements. This study tests the hypothesis that the *Deckenschotter* (high-level gravels), previously interpreted as purely fluvial, instead record a mixed delta-fluvial system developed within a partly lake-filled valley, driven by episodic damming and lake-level fluctuations. Integrated UAV photogrammetry, laser-scan mapping, sedimentary logging, granulometry, clast analysis and XRD methods are employed. Fieldwork reveals large-scale foresets, imbricated gravels and sedimentation cycles documenting north- and east-directed palaeoflow into the Salzach river, with gravelly delta fronts and sandy bottomsets punctuated by channel incision during base-level falls. These findings revise *Deckenschotter* models by demonstrating lacustrine influence prior to LGM glacier advance, implying widespread but previously unrecognised pre-LGM lakes across eastern Alpine valleys. Damming mechanisms such as moraine collapse, mass movements or alluvial fans from tributary valleys account for repeated transgressions-regressions, facilitating palaeoenvironmental reconstruction. Beyond Quaternary stratigraphy, the results inform geohazard assessment in inhabited Alpine settings by clarifying sedimentary architecture beneath active landslides, guiding future stabilisation efforts.

1.2 Geographical setting

Covering an area of approximately 11 km^2, whereby the elevation ranges between 1200 m.a.s.l in the south and roundabout 670 m.a.s.l. in the north (Figure 1A), the study area is located 60 km southwest of the city of Salzburg (Figure 1B) within the east-west running Salzach Valley. The study area, also known as Embacher Plaike (Plaike or Blaike is a salzburgian dialect expression for landslide), is defined by the Salzach River in the north, the village of Taxenbach and the Rauriser Valley in the west and the Gasteiner Valley in the east. The southern border of the site is represented by the northernmost foothills of the mountains Hörndl (1630 m.a.s.l.) and Brunntalköpfl (1591 m.a.s.l.) (Figure 1A, 1C). Several rivulets are running through the area, draining northeastwards into the Salzach.

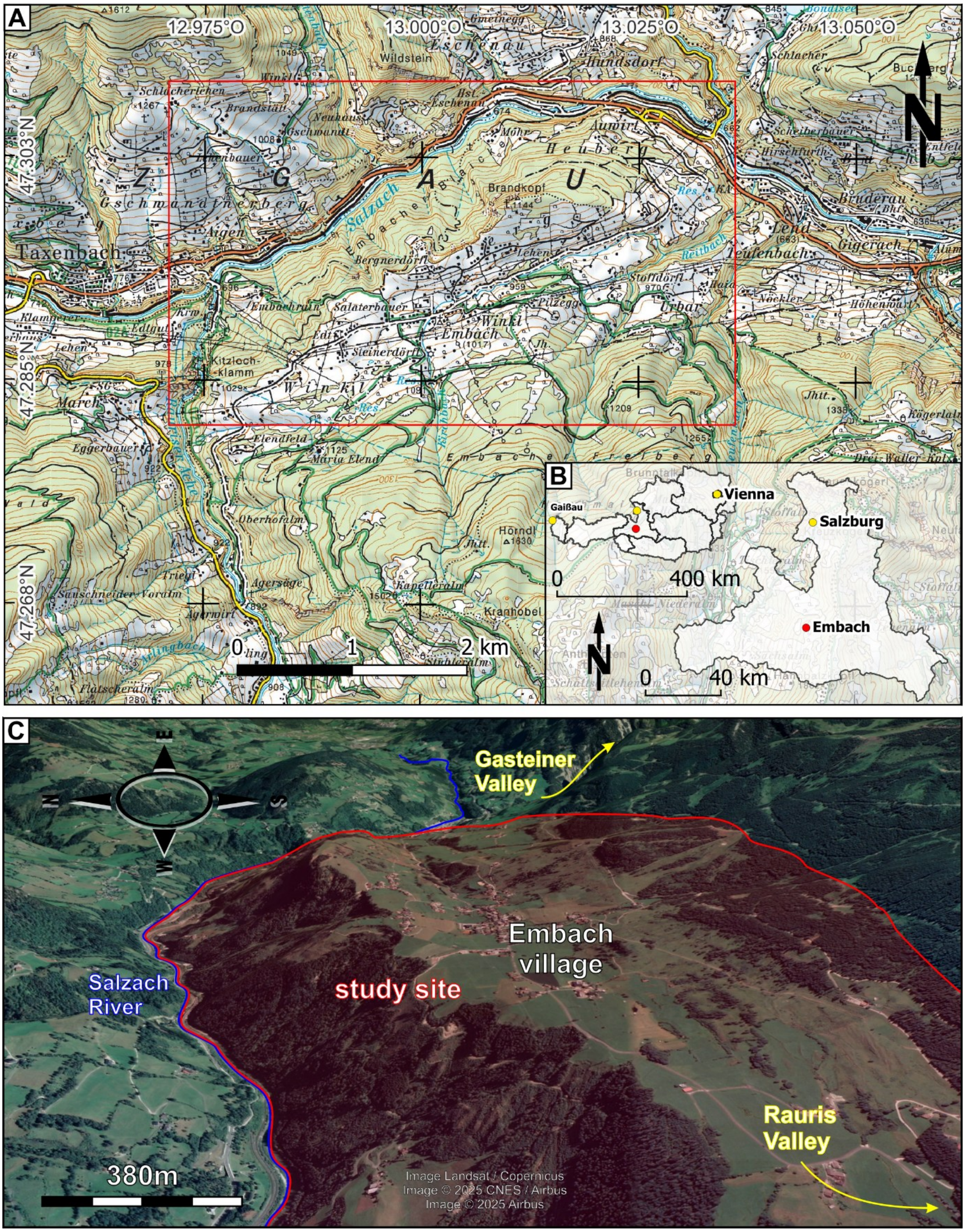

Figure 1: (A) topographic map showing the study area in the red rectangle, modified after BEV (2022); (B) location of the site within Austria (top left) and within the province of Salzburg; (C) oblique Google Earth perspective illustrating the borders of the study site, modified after Google Earth (2025)

1.3 Geological setting

1.3.1 Metamorphic Bedrock Evolution in the Salzach Area

The Salzach Valley is a very prominent E-W oriented structure in the eastern Alps. It forms part of the Salzach-Ennstal-Mariazell-Puchberg (SEMP) fault system, a major 400-km-long strike-slip fault zone that accommodated significant eastward extrusion of the Eastern Alps during Oligocene to Miocene north-south shortening (Frost et al., 2009). The bedrock around the Salzach region belongs to the Austroalpine crystalline units (Figure 2), chronicling a high-grade petrogenesis of metamorphic rocks during the Alpine orogeny. The Salzach area exhibits structurally complex nappe stacks, including parts of the Altkristallin, indicative of multiple phases of tectonic imbrication and regional metamorphism. This evolution relates to subduction, crustal thickening, and exhumation in the Eastern Alps (Groß et al., 2020; Schmid et al., 2013).

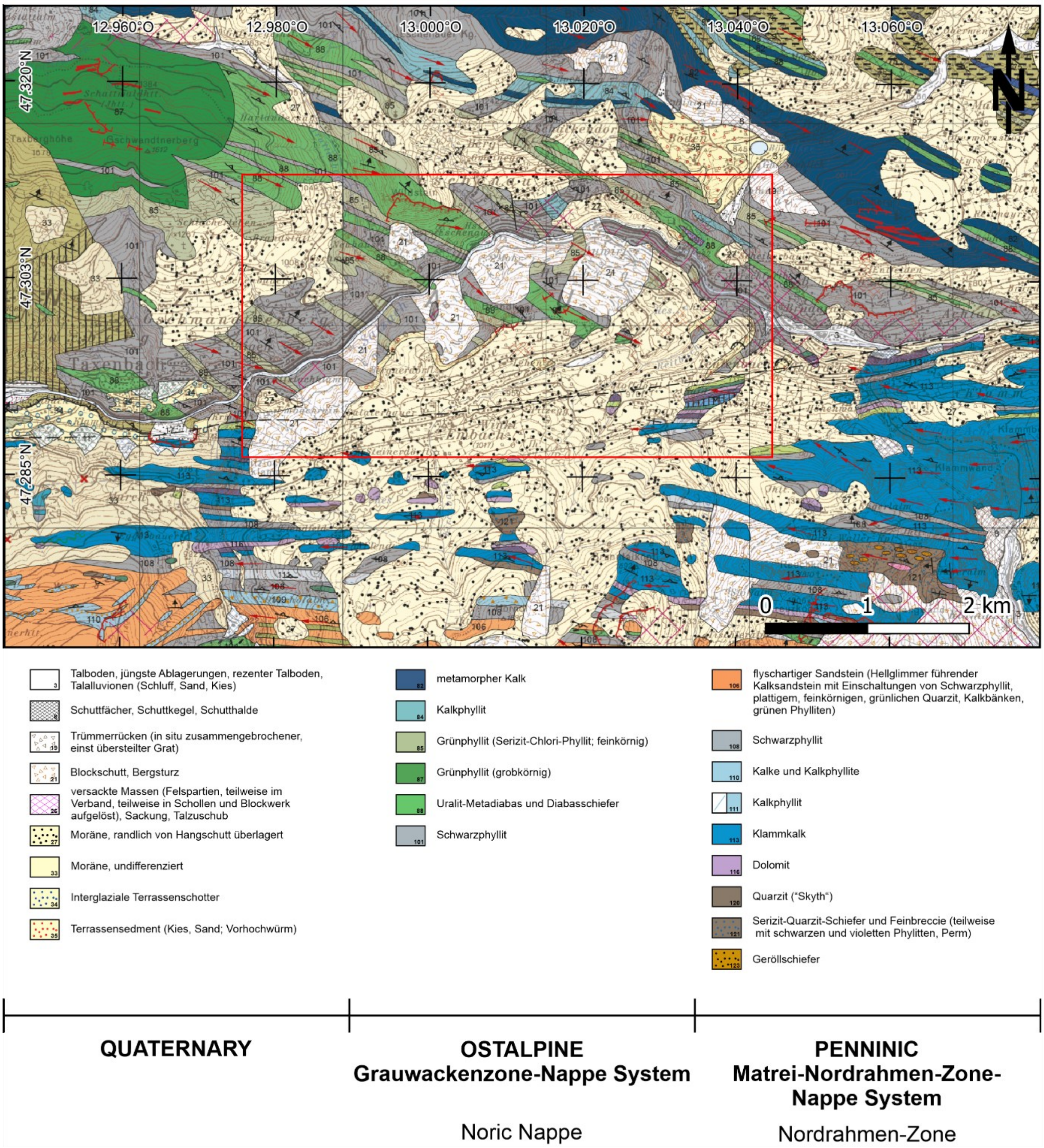

Figure 2: Geological map of the study area (red rectangle) and tectonic classification of lithologies modified after Kreuss (2013)

1.3.2 Quaternary Glaciation and Hanging Glaciers

The four major glaciations, Günz, Mindel, Riss and Würm, which shaped the present landscape of Austria, occurred during the Quaternary period (starting 2.58 Ma ago) whereat Würm glaciation (29 -12 Ka) is the most recent one (Reitner, 2022). During these successive glacial phases, the SEMP fault system was fully exploited as a structural weakness, principally by the Salzach Glacier. This was a trunk glacier dominating the Salzach Valley which, at peak thickness, exceeded 1.5 km, overdeepening the valley and depositing till and interfingering glaciofluvial outwash units, before terminating as a piedmont lobe in the Alpine foreland to the north (Reitner, 2022; Salcher et al., 2015; Van Husen, 2000). The overdeepened Salzach Valley basins thus record complex incisions during the Mindel, Riss and Würm (Last Glacial Maximum, LGM 30 - 18 Ka) glacial cycles (Ivy-Ochs et al., 2008; B. Salcher et al., 2024). Approximately 70 km east of the study area (Embach), Le Heron et al. (2023) and Griesmeier et al. (2025) showed that local blockage of the neighbouring Enns Valley took place, probably through the development of alluvial fans, to form a major lake prior to the LGM. This enabled them to reinterpret parts of the sand and gravel stratigraphy of the so-called *Deckenschotter* unit as lacustrine in origin. Consequently, this raises the possibility that similar, previously undocumented lake systems may have existed in other parts of the eastern Alps prior to the LGM. In the Salzach area, the trunk glacier probably also received material from hanging glaciers that were common on the steep valley sides in tributary valleys feeding into the Salzach Glacier. These glaciers developed where smaller tributary icy accumulations perched high on mountain walls descended partly but did not reach the main glacier surface, terminating abruptly at cliffs. These hanging glaciers were important contributors of rockfall material into the glacier valley below, and thus for fluvial sediment.

1.4 Previous research in the study area

In addition to geological mapping of the area, previous work has focussed on two key themes, namely (i) description of the mass movement processes and (ii) hydrogeological models pertaining to the mass movement.

1.4.1 Mass movement

Mass movements in the Embach area have been documented for centuries (Schroll, 1798) and intensely studied by Dietrich (1990). The excellent exposures of Quaternary sands and gravels owe their existence to a steep, receding scarp. Dietrich (1990) undertook a detailed study integrating preexisting (historical) data (e.g. expert's reports, construction documentations, well data and logs, extenso- and inclinometer data) with original field data, geological maps and engineering geological approaches. He argued that that origins of the mass movement could be attributed to (i) low shear-resistance of the substrate (heavily weathered phyllites) due to the transformation of sericite into hydromuscovite along their foliation plane, (ii) readily eroded sediments with a low mechanical strength further weakened by groundwater or rainfall, thus a receding scarp and (iii) erosion of the bedrock and valley deepening by Salzach river.

Dietrich (1990) also recognised the potential impacts of the ongoing gravitational instability for local communities, and summarised four measures that were taken in the preceding decades to counter the problem. These were (i) construction of gabion walls and drainage systems in the footwall of the Embacher Blaike in the 1940s, (ii) watertight enclosure of the rivulets Kirch- and Salaterbach to reduce water intruding the sediments in the 1970s, (iii) reforestation of the upper part of the slopes to stabilise sediments and (iv) construction of a groundsel in the riverbed of the Salzach to stop erosion and valley deepening.

1.4.2 Hydrogeology of the mass movement

In this area, the work of Brandner (2017) is the most recent, focussing on the hydrogeology of the mass movement.

Their four key findings include (i) considerable differences in electrical conductivity of the Embacher Plaike and the orographic catchment area of the rivulets Kirch- and Salaterbach, based on varying sulphate contents in the underground, (ii) effluent flow behaviour of the Kirchbach, shown by discharge measurements, (iii) tracer analysis indicates no connection of Embacher Plaike and the rivulets on the plateau and (iv) a water balance for the catchment area of the Plaike was calculated, showing that the calculated discharge exceeds the real measured discharge.

These results show that very little to no connection of the Embacher Plaike and the rivulets, respectively the plateau, is given and therefore the Plaike and the rivulets have independent hydrogeological systems. Thus, the interpretations of Brandner (2017) would appear to overturn the earlier assumption (Dietrich, 1990; and references therein) that the Kirch- and Salaterbach streams feed groundwater and thus promote mass movement.

2 Methods

2.1 Fieldwork / Data collection

The fieldwork was conducted during two campaigns, one in November 2024 and a second in May 2025. During these campaigns, classic sedimentological field methods were used to describe the outcrops and gain data. Additionally, several drone flights were undertaken and a total of 12 samples were collected. Detailed descriptions of the methods applied are provided herein.

2.1.1 Sedimentary logging

The profiles shown in chapter 3.2 were derived from outcrop EMB1A during November 2024 to facilitate the description of the sediment and to distinguish different sedimentological facies distributed over the outcrops. Later on, they were digitised using CorelDRAW 2021. These five profiles are the only ones that were drawn in detail, as the other outcrops did not allow a closer examination regarding the ongoing erosional processes, e.g. rockfalls.

The profiles are named after the outcrop (EMB1A), followed by the letter P for 'profile' and then numbered from 1 to 5 to ensure a consistent labelling, e.g. EMB1AP3. The logs are drawn in scale 1:10 with the exception of profile EMB1AP1 which is drawn in 1:20 facilitating graphical display.

During the logging, information on lithological variations, grain size distributions, sedimentary structures, colours of the sediment and sedimentary contacts were obtained, simultaneously noted and then graphically displayed. Additionally, the precise locations of the samples taken were marked, as well as the data of different measurements.

2.1.2 Measurements

Whilst studying the outcrops, cross beddings and imbrications were measured, displaying the data as dip and dip direction and plotted as great circles in a stereographic net. The measurements were then also plotted as rose diagrams for directional analysis. For plotting the great circles Stereonet 11 (Allmendinger, 2024) and for the directional analysis OpenStereo 2.0 (Grohmann, 2025) were used.

The orientation of drumlins, obtained from the geomorphological map described in chapter 2.4 and 3.1.1, were measured digitally in CorelDraw. The geomorphological map was imported into CorelDraw, then the angle of the longest axis of the drumlins was measured, allowing glacier flow to be inferred. The measurements and corresponding figures are shown in chapter 3.1.1 and 3.5.

2.1.3 Sampling

During the fieldwork, approximately 34 kg of material, divided among 13 samples (Table 1), were taken from the outcrops EMB1A, EMB3, EMB4A and EMB4B. The nomenclature of the samples follows the same scheme as for the profiles mentioned above, using the letter S instead of the letter P, e.g. EMB1S1. The samples were then used for different analyses, see chapters 2.5 – 2.7.

Table 1: list of samples taken during both field campaigns and type of analyses applied

	SAMPLE N°	**TOTAL WEIGHT [g]**	**ANALYSES**		
1	EMB1AS1	14887,800		XRD	CLAST ANALYSIS
2	EMB1AS2	1838,354			
3	EMB1AS3	1909,851			
4	EMB1AS4	1112,645			
5	EMB1AS5	781,693	SIEVING		
6	EMB1AS6	923,495			
7	EMB1AS10	3440,900	SIEVING	XRD	
8	EMB1AS12A	741,204	SIEVING		
9	EMB1AS12B	2433,600	SIEVING	XRD	
10	EMB3S1	1221,000	SIEVING	XRD	
11	EMB3S2	4684,400	SIEVING	XRD	
12	EMB4BS1	21230,000			CLAST ANALYSIS
13	EMB4BS2	1480,885	SIEVING	XRD	

2.1.4 Uncrewed Aerial Vehicle - UAV

Photogrammetry is now a standard approach in field geology, and the aim was to capture the 3D geometry of the outcrops for later analysis (mapping of facies and facies boundaries) in the laboratory. To achieve this, 1304 photographs were taken by a DJI Mavic Mini 4 UAV during November 2024 and May 2025. The drone was flown manually in double grid configuration across the outcrops, taking pictures with an overlap of 60 – 70 %, and thus enabling high resolution 3D models and orthomosaics.

2.2 Photogrammetry workflow and image processing

Production of 3D photogrammetric models was undertaken in Agisoft Metashape Professional v2.1.3 (*Metashape*, 2024). The following workflow was applied to all the datasets of the outcrops EMB1A, EMB2A, EMB2B, EMB2C and EMB3.

(1) Adding all the pictures for the respective outcrop
(2) Aligning the pictures, resulting in Tie Points
(3) Point Cloud generation Building Model
(4) Building Texture, resulting in textured 3D Model
(5) Building and exporting an Orthomosaic

2.3 Sequence stratigraphy

The sequence stratigraphic approach follows that undertaken by Le Heron et al. (2023) on pre-LGM sands and gravels of the Grobminger Mitterberg, Ennstal. This involved the generation of a chronostratigraphic chart or Wheeler diagram (Emery & Bertram, 1996). The extracted orthophoto of the EMB1A 3D model was imported into CorelDraw where the first step, distinction between different facies, was done by highlighting these areas in different colours. Secondly, the orthopicture was studied in detail, to determine the lateral extent of beds, each interpreted as a different sedimentary event, and thus representing different time intervals. Next, the lateral extent of beds was plotted as bars beneath the orthomosaic, in the respective colour of the facies, limited by the lateral extension of these lines as seen on the orthomosaic.

Additionally, a relative lake level curve was constructed on the basis of stratal geometries to infer phases of transgression and regression, and thereby reconstruct base level.

2.4 Geomorphological mapping

In order to set the Embach outcrops into a wider context of Quaternary glaciation, the surrounding area was mapped, focussing on geomorphological features. Mapping was undertaken on freely available 1 m resolution laser scan data from Land Salzburg (2017). This was performed in the geoinformation system QGIS 3.42.3 using the MGI / Austria GK M31 (EPSG: 31258) projection. Contours of drumlins were mapped as well as the scarp of the landslide by using lines for the scarp, points for the outcrops and polygons for the drumlins.

2.5 Granulometry / Sieving and Sedigraph

Depending on the grain size of the samples, different methods were chosen for grain size analysis. These were: dry sieving of the gravel samples for grain sizes (64 mm to 2 mm), wet sieving of the sand fractions (2 mm to 0.063 mm) and analysis via Sedigraph for the silt and clay fractions (0.063 mm to 0.002 mm). Care was taken to ensure maximum accuracy of measurement according to the following workflow:

(1) After drying the samples in the oven at 65 °C, they were weighed and dry sieved. This was done with a sieving machine where the sieves with mesh sizes of > 64 mm, > 32 mm, > 16 mm, > 8 mm, > 4 mm, > 2 mm and a bowl collecting the < 2mm fraction, were placed upon. This first step was then finished by weighing all the different fractions

(2) In the second step, the < 2 mm fraction was divided via a Riffle splitter several times to obtain representative quantities (~70 g – 200 g) for the wet sieving, which were also weighed.

(3) Thirdly, 200 ml of a 15 % H_2O_2 solution was added to the samples to remove the organic matter.

(4) After letting the samples react for five days, the samples were then further disaggregated with an ultrasonic probe at 400 W for four minutes and finally wet sieved. For that, sieves of > 1 mm, > 0.5 mm, > 0.25 mm, > 0.125 mm, > 0.063 mm sized meshes were used. The < 0.063 mm fractions were collected during this process for further analysis with the Sedigraph.
(5) The next step was to dry the obtained grain size fractions in the oven again and subsequent weighing.
(6) Using the Micromeritics Sedigraph III 5125, approximately 2 g of the < 0.063 mm fraction of each sample were taken for analysing the grain size distribution, leading to mass percentages of the grain size fractions > 0.032 mm, > 0.016 mm, > 0.008 mm, > 0.004 mm, > 0.002 mm and < 0.002 mm. To avoid coagulation, the samples were mixed with 0.05 % sodium tripolyphosphate ($Na_5P_3O_{10}$) before analysis.

For grain size fractions smaller than 0.0063 mm the sedigraph was used which determines the sedimentation velocities of the particles and thereby measures the particle sizes. This phenomenon is based on Stoke's law whereas the determination of the mass concentrations is based on the Beer-Lambert-Bouger law. Though, the absorption of the X-ray beam going through the fraction of the sample in suspension is measured (Boggs, 2006; „Sedigraph III Plus", (n.d.)).

Ultimately, the data were plotted and grain size distribution curves could be constructed. These steps were applied to all eight samples, listed in the table below.

Table 2: list of samples and sample weights used for sieving and sedigraph analysis

	SAMPLE N°	**WEIGHT [g]**	**ANALYSES**	
1	EMB1AS1	69.00	SIEVING	SEDIGRAPH
2	EMB1AS5	215.80	SIEVING	SEDIGRAPH
3	EMB1AS10	194.10	SIEVING	SEDIGRAPH
4	EMB1AS12A	205.00	SIEVING	SEDIGRAPH
5	EMB1AS12B	145.9	SIEVING	SEDIGRAPH
6	EMB3S1	63.78	SIEVING	SEDIGRAPH
8	EMB3S2	69.98	SIEVING	SEDIGRAPH
7	EMB4BS2	20.59	SIEVING	SEDIGRAPH

2.6 Clast analysis

Clast analysis was conducted to provide a broader regional geological context and to place better constraints of the depositional process. Hence, 65 randomly selected clasts out of two samples, namely EMB1AS1 and EMB4BS1, were analysed based on the length of their orthogonal a-, b-, and c-axis, whereas a is the longest, c the shortest and b the intermediate axis of the clast. Additionally, the angularity was assessed and class-divided into angular (A), subangular (SA), subrounded (SR) and rounded (R). Furthermore, the lithology was determined, as well as the presence of faceting, scratches or striations were noted.

After that, the data was plotted in Tri-Plots (Graham & Midgley, 2000; Sneed & Folk, 1958) which allow comparison of different depositional environments, based on the ratios of the clast's axis. One major attribute of these Tri-Plots is the so-called C40-line which indicates the threshold where the ratio of c:a axis is 0.4, meaning that the clast develops a more elongated shape. This yields information on transportation processes, as clasts transported subglacially tend to be more elongated than, e.g. fluvial transported clasts, therefore having greater c:a ratios (Benn & Ballantyne, 1994).

The shape of the clasts is not only affected by sedimentological processes but also by their lithologies. Different lithologies may behave differently within the same kind of transport, erosion or deposition, which is crucial to understand when interpreting data obtained therefrom (Lukas et al., 2013).

2.7 XRD

Bulk mineral composition, combined with lithological analysis of chapter 2.6, also facilitates a more detailed conclusion on the source of the sediments. Consequently, powdered samples were prepared from the < 0.063 mm fraction of samples EMB1AS1, EMB1S10, EMB1AS12B, EMB3S1 EMB3S2 and EMB4BS2 to analyse them with X-ray diffraction (XRD). XRD is an analytical method to identify minerals and is based on Bragg's law which characterises the interdependence between X-ray wavelength (λ), distance between atomic crystal planes (d) and angle of diffraction (2θ):

$$n\lambda = 2\,d\,sin(\theta)$$

n ... order of diffraction maximum, λ … X-ray wavelength, d … space of crystal planes, θ … diffraction angle

The finely ground powder was placed into the sample holder using the backloading procedure. The top of the sample holder is clamped into the device and then filled, whereby the powder must be added precisely and sufficiently and afterwards it gets pressed down. Finally, the back of the sample holder is added (Perkins, 2025).

The measurements were carried out with a Panalytical X'Pert PRO X-ray diffractometer which uses CuK_α radiation, operates at 40 kV and 40 mA at a step size of 0.0167 ° and 5 s per step between 0 ° and 70 ° 2θ. For final qualitative identification of the mineral phases, the PANALYTICAL programs X'Pert Data Viewer and X'Pert HighScore Plus were used.

3 Results

3.1 Geomorphological mapping

Geomorphological mapping revealed subglacial channels and 15 drumlins (Figure 3). Drumlins were mapped as turquoise planes encircling the structures identified on the hillshade. The subglacial channel was drawn as a purple line. Additionally, the current scarp of the mass movement (red line), as well as the locations of the outcrops (yellow stars) are marked, which will be described in more detail in chapter 3.2. For better orientation, the west-east running Salzach and its tributaries are mapped in dark blue.

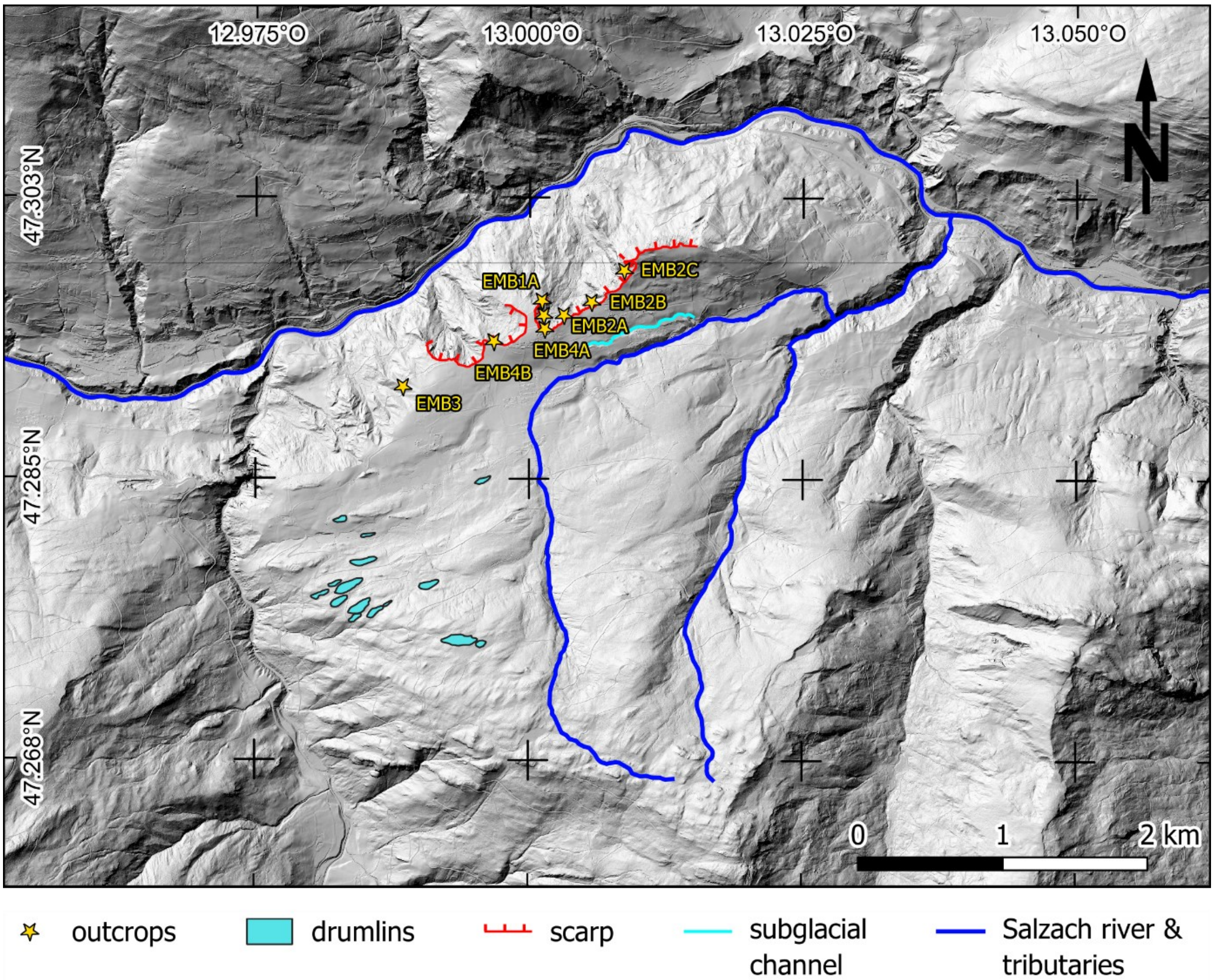

Figure 3: Geomorphological map of the study area with highlighted subglacial features, main scarp and outcrops (EMB1B is located between EMB1A and EMB4A)

3.1.1 Drumlins

The data of the geomorphological map in chapter 3.1, directions of the drumlins respectively, are shown in Figure 4. The general direction stands in contrast to the data of the foresets and imbrications (chapter 3.5), as the drumlins are going to the East-North-East (ENE) with an angle of 69.20 °.

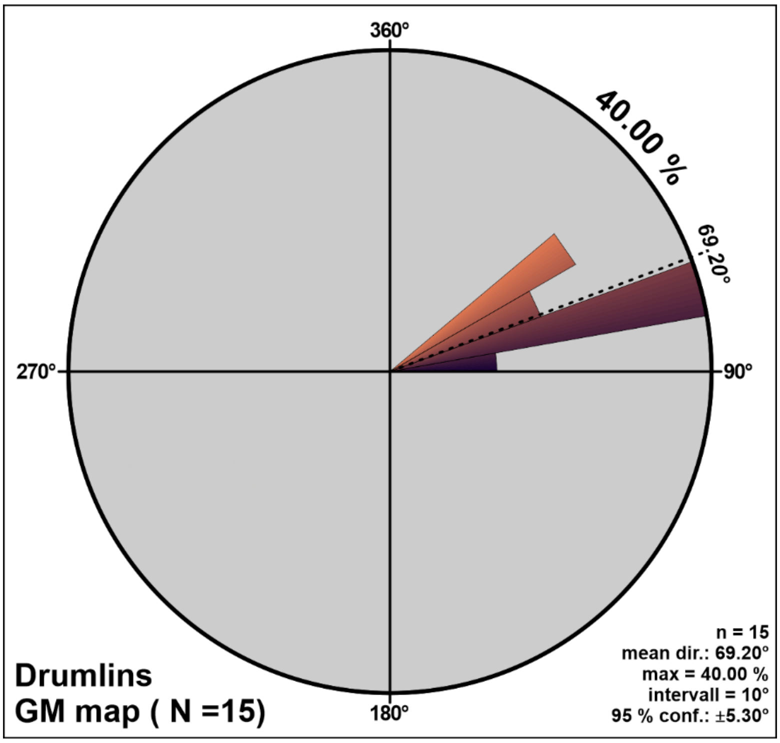

Figure 4: rose diagram of 15 measured drumlins, general direction ENE (69.20 °)

3.2 Geological observations

The Pleistocene sedimentary succession exposed at Embach, Salzburg, Austria, consists of a 760 m long and ca. 45 m high scarp and is divided into the outcrops EMB1A-EMB4 (Figure 5).

Figure 5: (A & B) overview drone pictures of the section with indicated locations of the outcrops and distribution of till, sands and gravels

The strata consist of an approximately 40 m thick vertical sequence of interbedded sands and gravels, documented in detail using digital outcrop models and sedimentary logs (Figures 6, 13, 14, 15). Grain sizes throughout the section vary systematically between silt (Si) to fine sand (fS), coarse sand (cS), and gravel fractions classified as fine gravel (fGr), gravel (Gr), and coarse gravel (cGr), illustrating vertical and lateral heterogeneity in sediment texture respectively. Sedimentary structures observed in the succession include dominantly subhorizontal planar bedding and cross-bedding (Figures 6, 7, 8, 9D), with the overall assemblage strongly resembling that documented in Ennstal toward the east (Le Heron et al., 2023). Clast imbrication within gravel beds is locally well-developed (Figures 7C-D). Both clast-supported and matrix-supported gravel beds are present at different levels within the succession. The beds are of variable (cm- to m-scale) thickness and exhibit frequent interbedding of sand and gravel units, reflecting the complex layering documented in the sedimentary logs (Figures 13, 14, 15). The topmost deposits comprise ca. 15 m thick greyish-brownish layer of clast-rich, muddy diamicton (Figures 5, 9). This deposit is overconsolidated (Clarke, 2018) and most cm to m-scale clasts are striated (Figure 10). The diamicton thickens eastwards; in the western and middle part of the outcrop it is partially to completely eroded through slope failure. Products of recent slope instability are abundant in the lee of the scarp, including soft-sediment striated mudflows derived from the diamicton (Figures 5, 8) and debris fans (Figures 5, 7E-F). Locally, these cut the sediment layers described above discordantly.

In summary, the architecture of the Embach succession can be distilled as a complex interbedding of sands and gravels exhibiting diverse grain size distributions, bed thicknesses, and sedimentary structures, capped by a layer of diamicton.

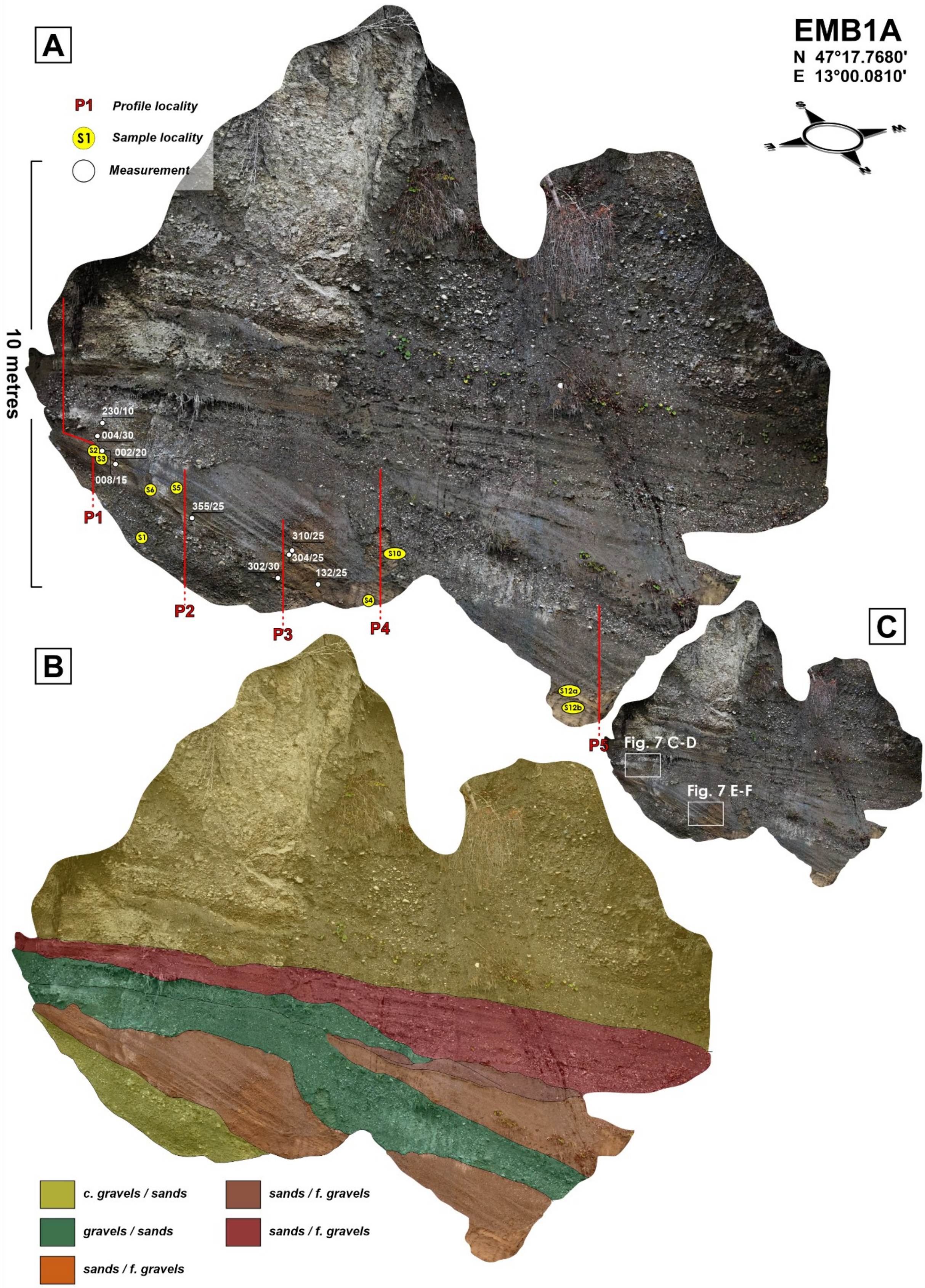

Figure 6: (A) orthomosaic of EMB1A, red lines indicate profile locations, yellow markers show sample locations and measurements in white (B) orthomosaic of EMB1A coloured according to different lithologies (C) orthomosaic of EMB1A showing locations of detailed photographs in Figures 7A-D

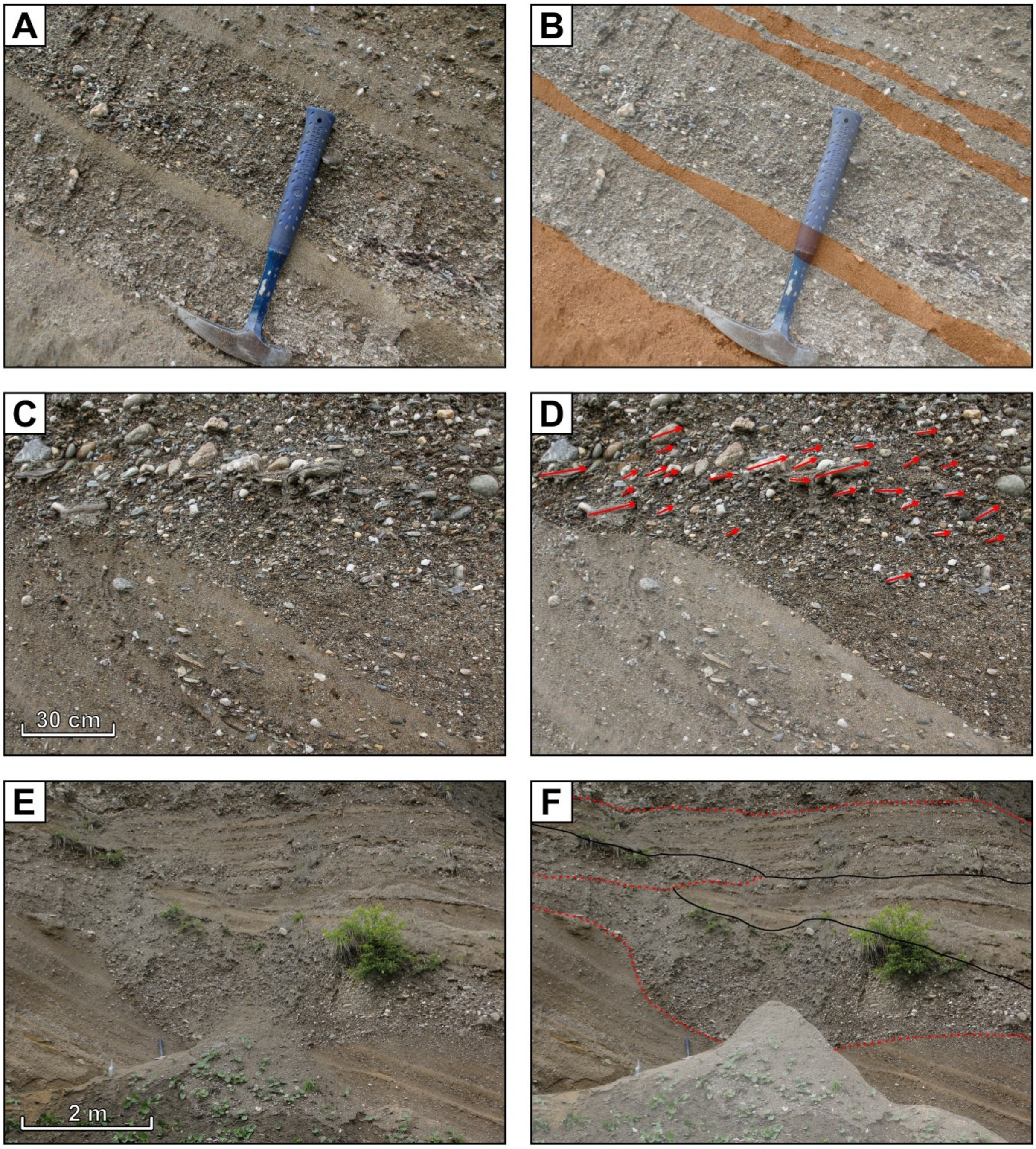

Figure 7: (A-B) layers of interbedded sands (orange) and gravels (white) at EMB1A (C-D) imbricated clasts of EMB1A, red arrows indicated flow direction (E-F) sedimentary architecture at EMB1A with highlighted erosional contacts (red dotted line)

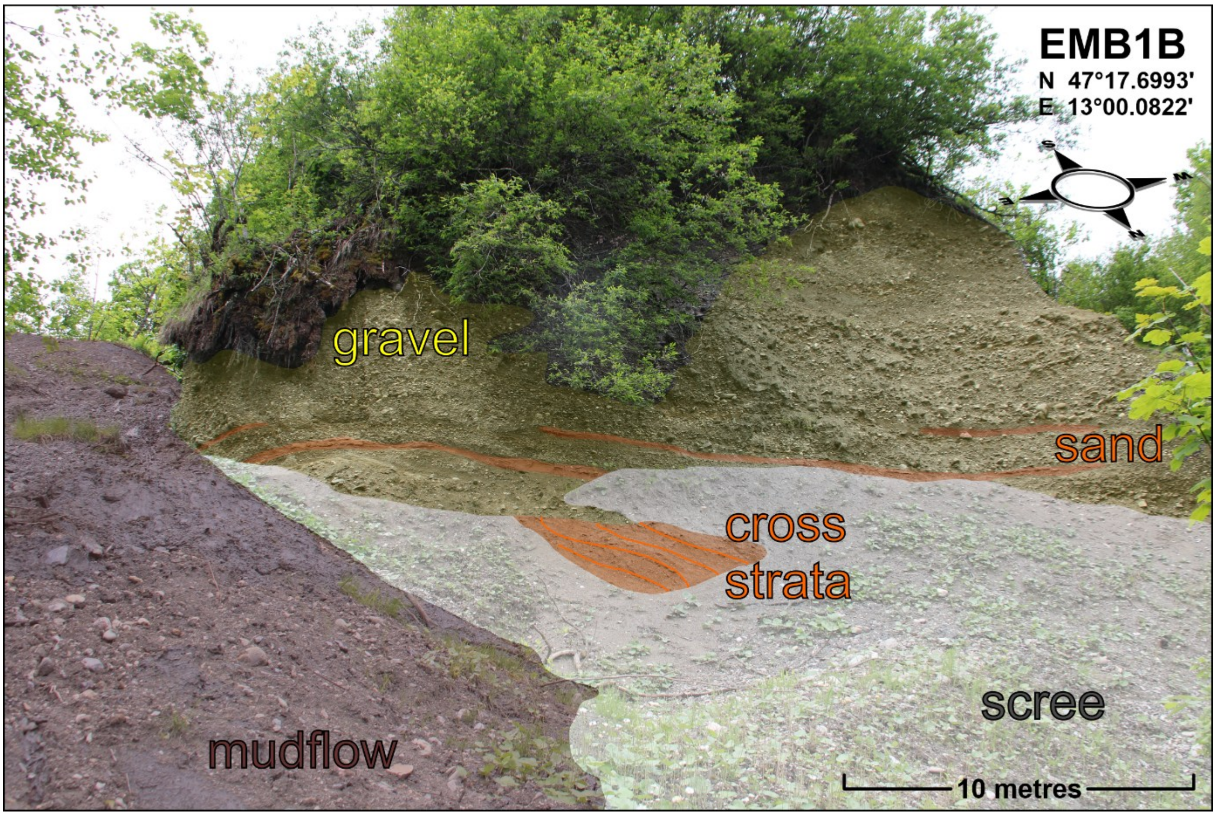

Figure 8: picture of EMB1B with indicated cross stratification (orange), gravel deposits (yellow) and recent mudflow (brownish)

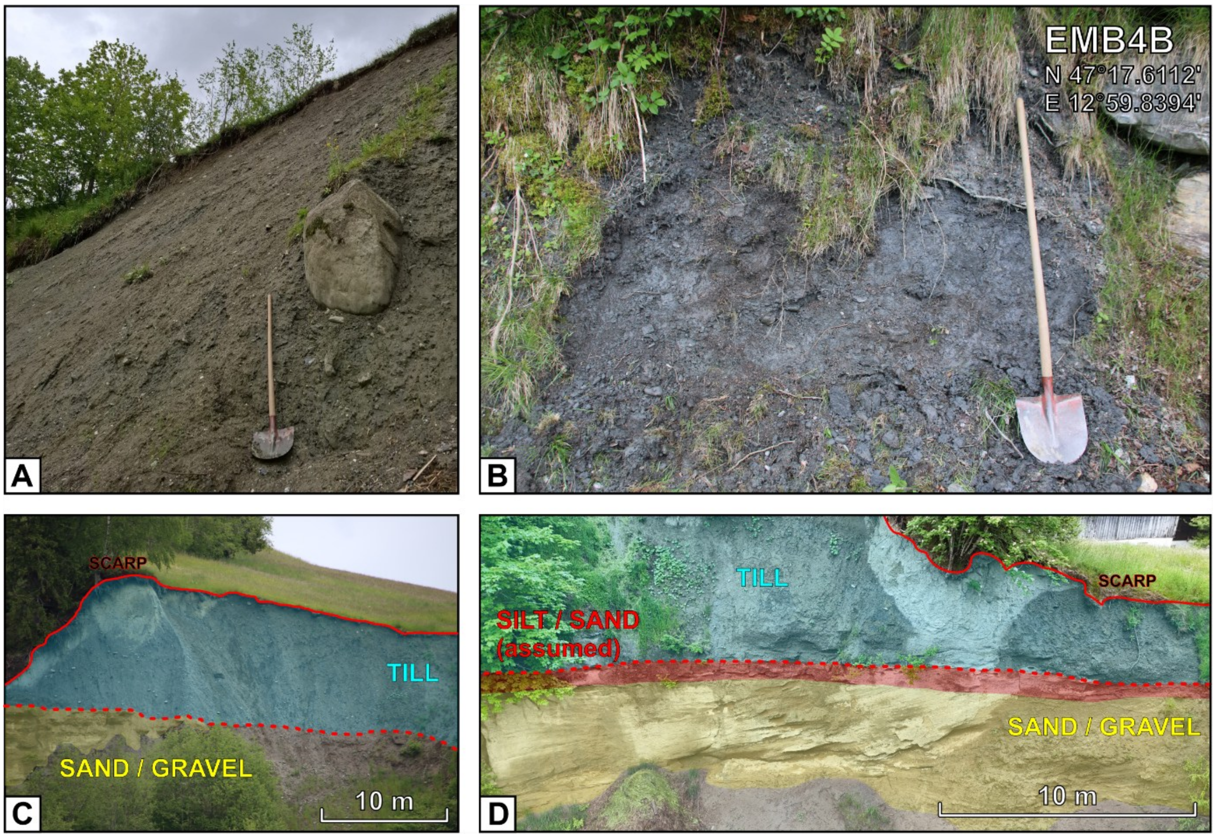

Figure 9: detailed photographs (A and B) and drone pictures (C and D) showing the position of till (blue) capping the sedimentary succession below (red and yellow)

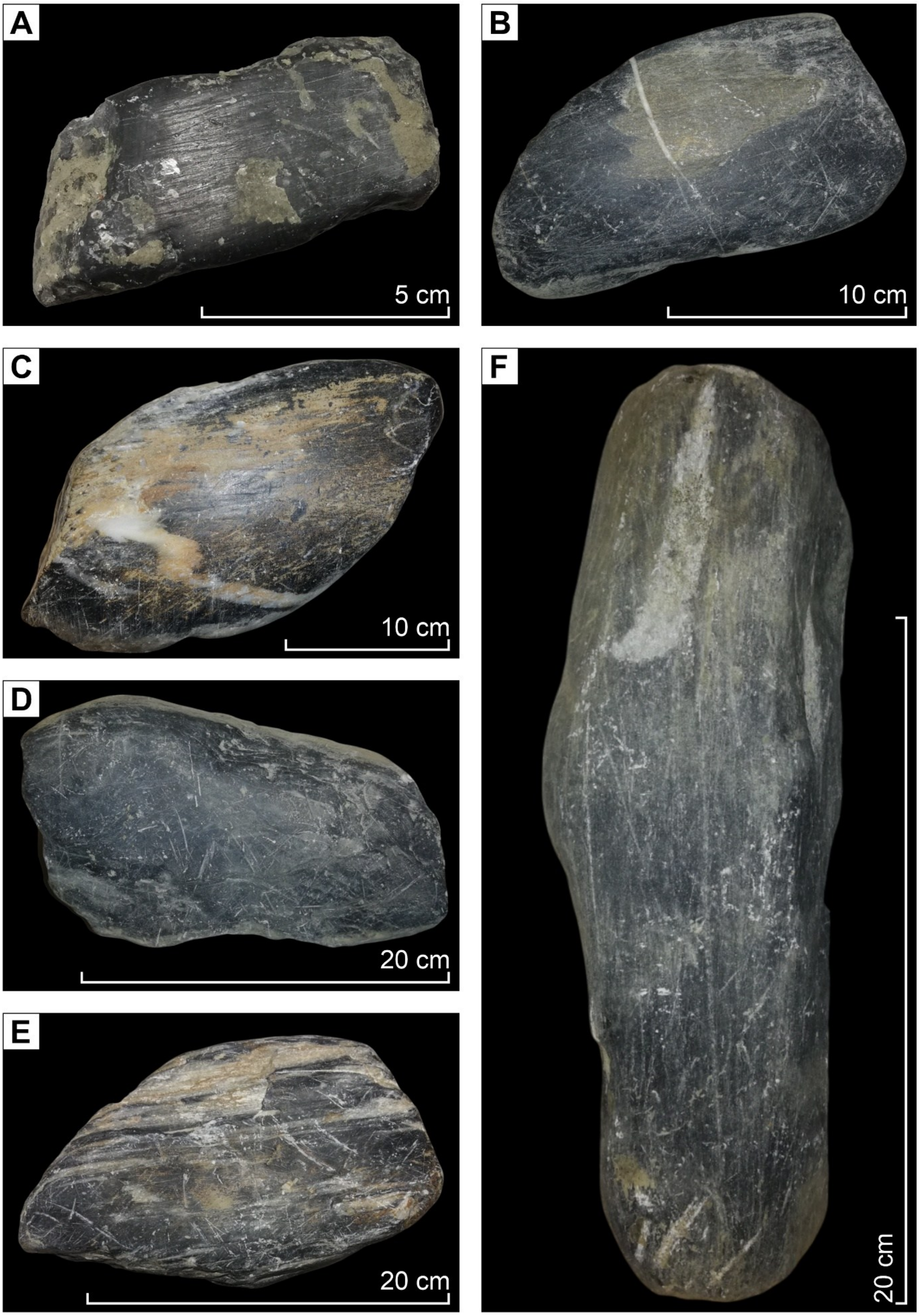

Figure 10: striated clasts of “Klammkalk” (mylonitic carbonate), sample EMB4*B*

In total, 65 clasts of the outcrops EMB1A (N = 26) and EMB4B (N = 39) were randomly picked. Six different lithologies were identified and their percentages are shown in Figures 11 and 12.

(1) Gneiss

(2) Quartzite

(3) Greenschist

(4) Klammkalk (Marble mylonite)

(5) Phyllite

(6) Lithic fragment

The sample of EMB1A (N = 26) mostly comprises gneisses (34.62 %), quartzites (26.92 %) and "Klammkalke" (marble mylonites) (23.08 %), with greenschists (11.54 %) and lithic fragments (3.85 %) playing a minor role and no phyllites were observed.

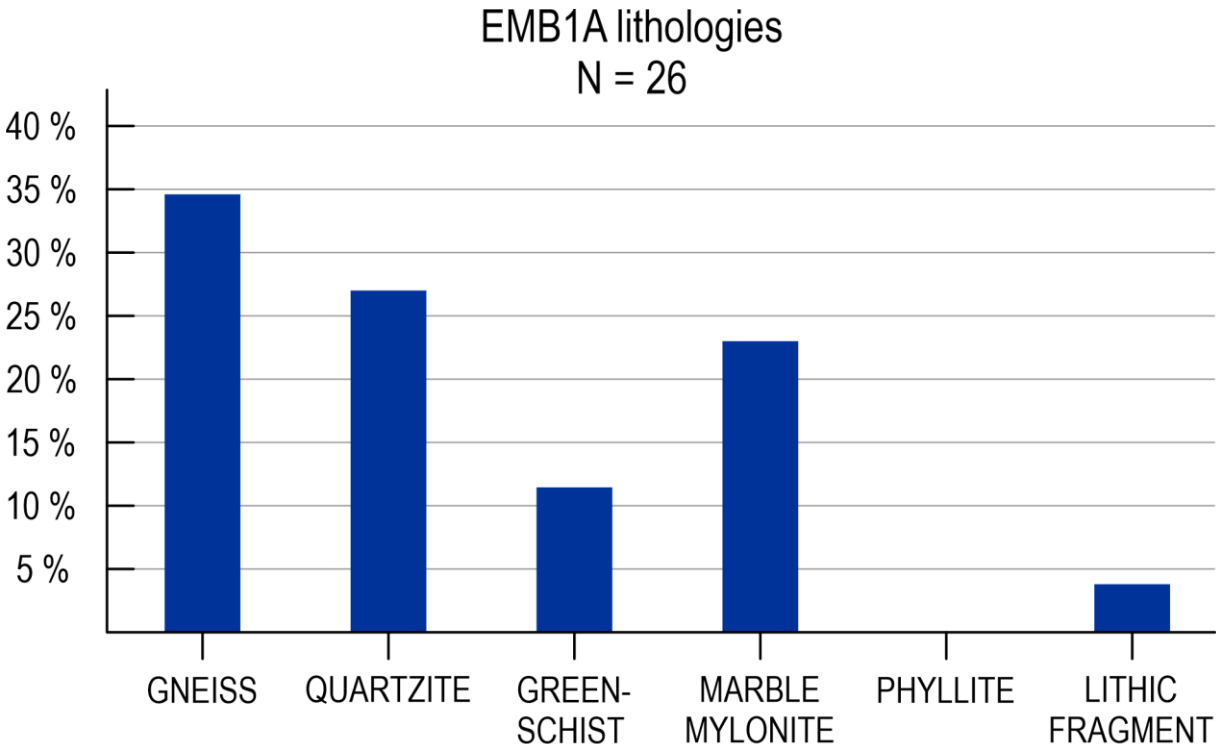

Figure 11: graph showing percentages of the lithologies, sample EMB1A

The predominant lithology of EMB4B (N = 39) with 69.23 % is Klammkalk, followed by phyllite (20.51 %), quartzite (7.69 %) and greenschist (2.56 %). Both, neither gneiss nor lithic fragments could be observed.

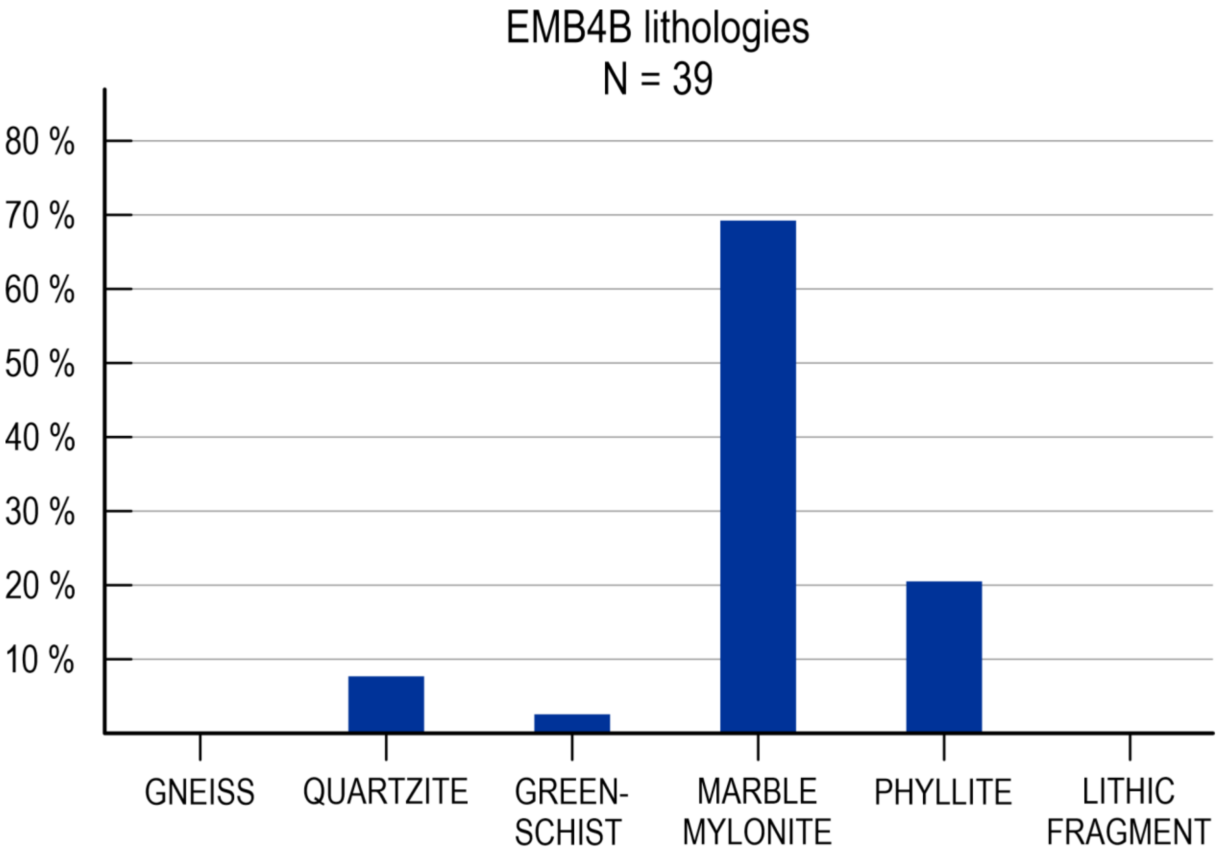

Figure 12: graph showing percentages of the lithologies, sample EMB4B

3.3 Profiles

Profile EMB1P1 (Figure 13) contains regularly alternating beds of gravels and sands. Beds here show subtle discordances and interbedding with thicknesses generally less than 20 cm per bed. Profile EMB1P2 (Figure 13) is characterized by coarser sediments, predominantly gravel, with bed thicknesses typically reaching up to 80 cm. Fining-upward sequences, where grain sizes progressively decrease upward within bed sets, are recorded. Profiles EMB1P3 and EMB1P4 (Figure 14) display a more variable facies assemblage with mixtures of clast- and matrix-supported gravels and sands. These profiles also show structures such as planar bedding, cross-bedding, and imbrication with bed thicknesses commonly ranging from 10 to 50 cm. Profile EMB1P5 (Figure 15) largely comprises gravel intervals interspersed with sandy beds. Beds occasionally show sharp boundaries, with thicknesses varying widely up to about 100 cm.

Fining-upward sequences are observed in several profiles interspersed with beds showing variable grain size and support, and occasional erosional discontinuities are noted interrupting the stratification. Matrix support within gravel-dominated beds fluctuates laterally and vertically through the logged successions. Subhorizontal bedding orientations are dominant, as revealed by the digital outcrop models and logs, providing detailed layering patterns and sediment texture structures across the profiles.

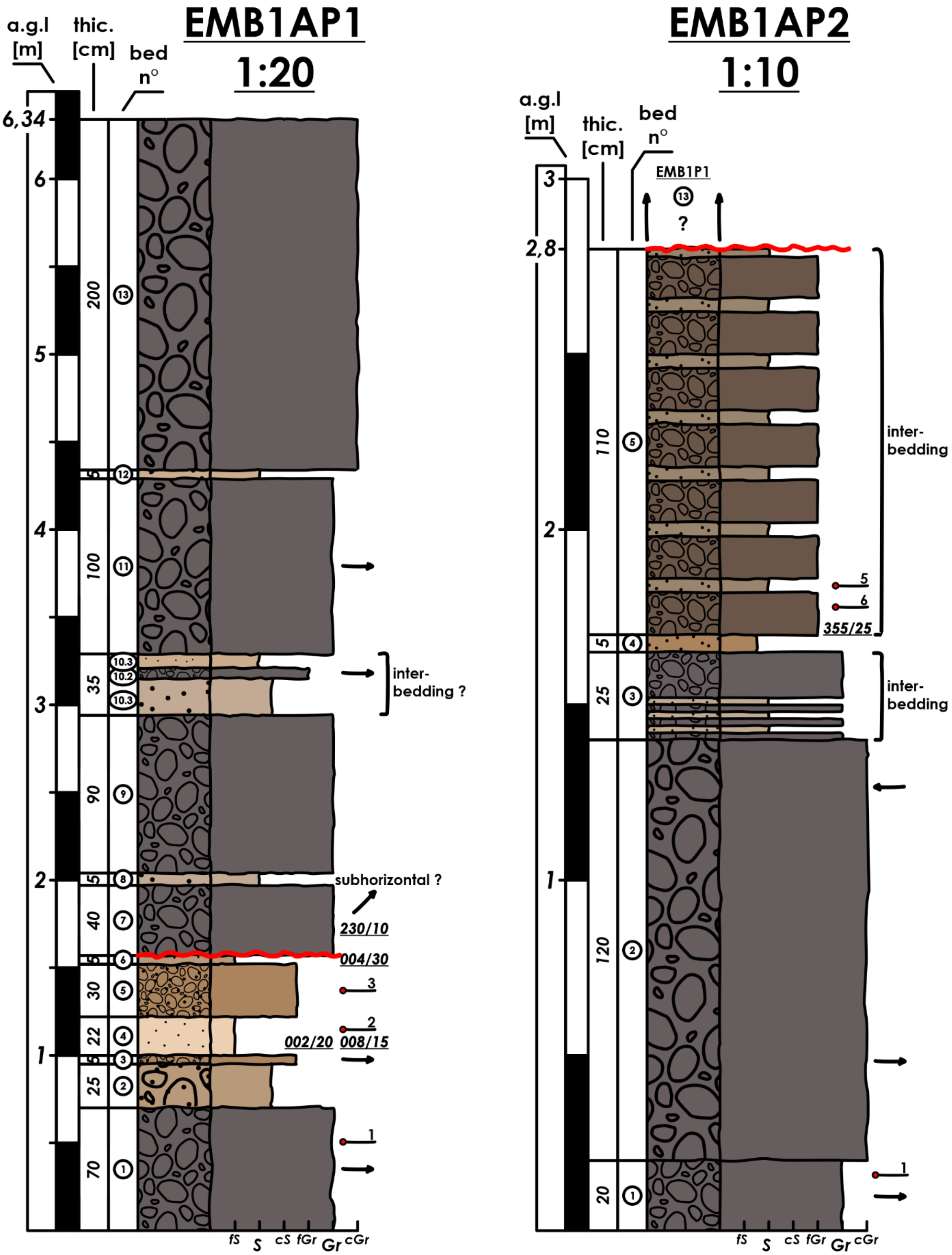

Figure 13: profiles 1 and 2 of outcrop EMB1A taken in the field

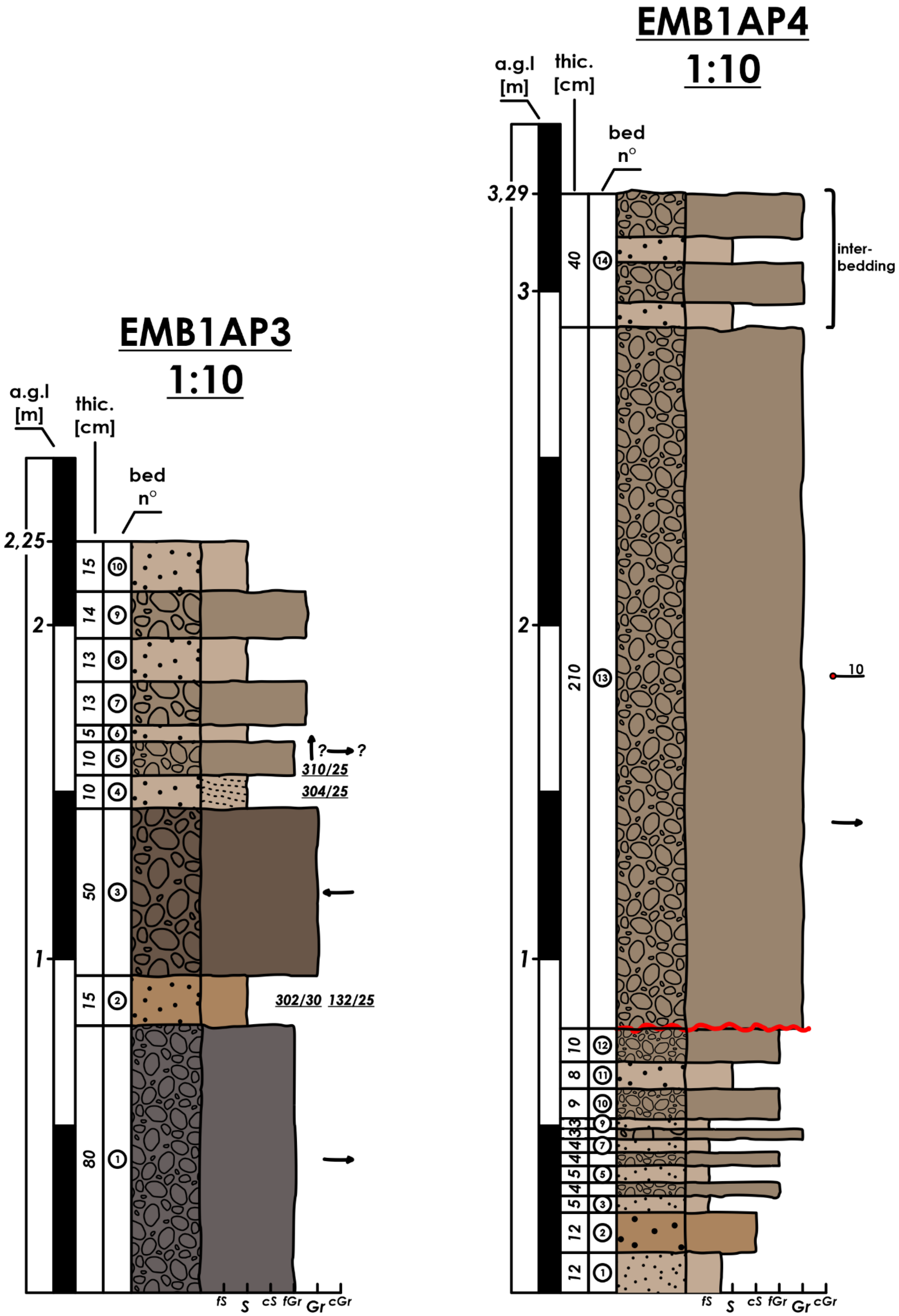

Figure 14: profiles 3 and 4 of outcrop EMB1A taken in the field;

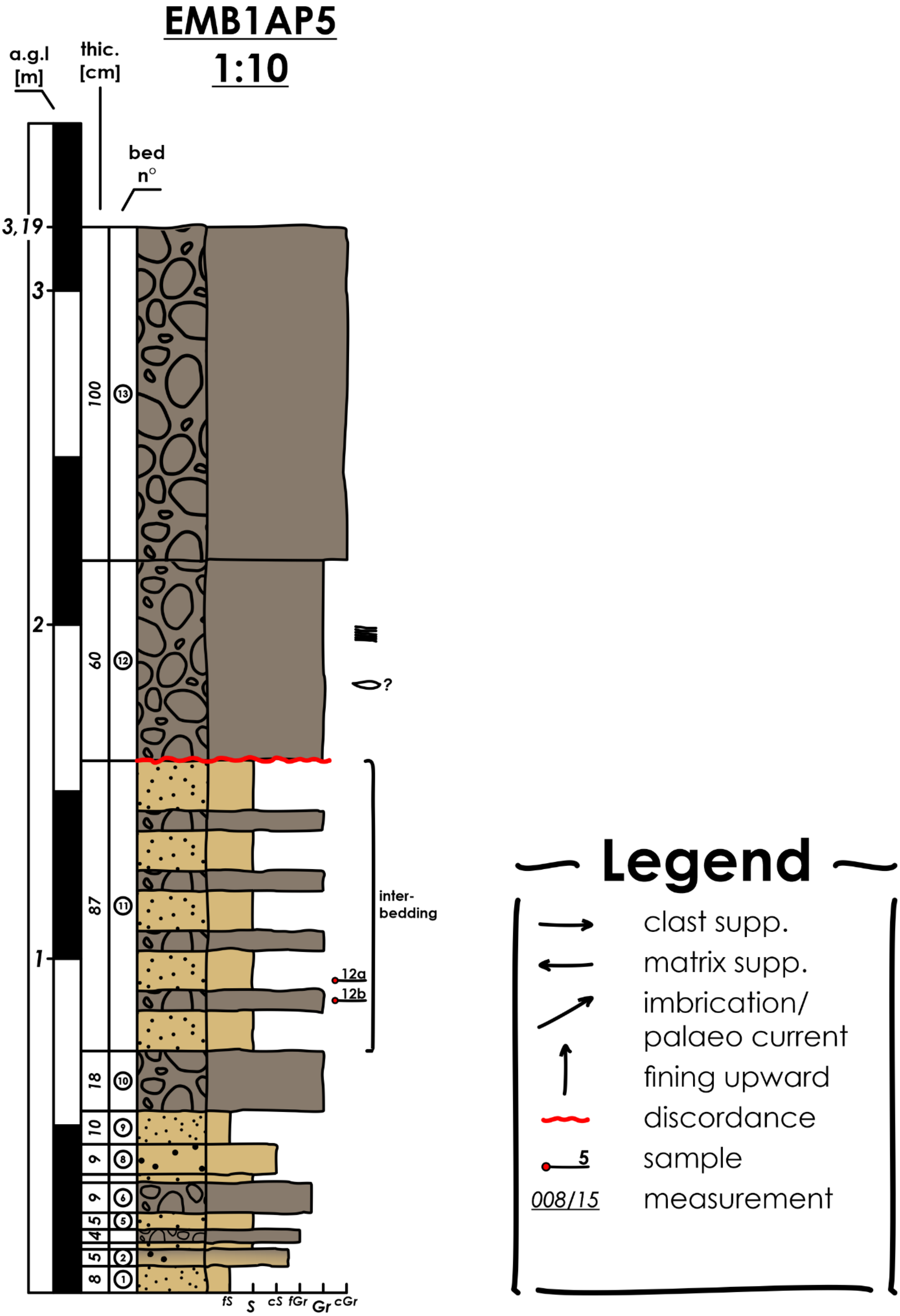

Figure 15: profile 5 of outcrop EMB1A taken in the field and legend for profiles

3.4 Sequence stratigraphy

The sequence stratigraphic approach led to a differentiation of five distinct sedimentary facies including (i) coarse gravels / sands (yellow), (ii) gravels / sands (green), (iii) cross stratified sands / fine gravels (orange), (iv) sands / fine gravels (brownish) showing ripple-like structure and (v) subhorizontal bedded sands / fine gravels (reddish) (Figure 16).

Based on the orthomosaic of EMB1A, a total of 33 individual sedimentary events could be identified, representing individual time steps. The intervals ("T") of T1 - T17 & T18 - T22(25) bear the cross stratified sands and fine gravels which are one of the most striking features of the outcrop. These two intervals were interrupted by a phase of gravel & sand sedimentation (T17 - T18) highlighted in green, and which lies discordantly (T17) on the lower cross bedded sand and fine gravel unit. A very similar situation occurs between T23 - T26, where a relatively thick bed of gravel and sand rests on top of the second sand / fine gravel interval of T18 - T22(25). The penultimate unit (T26 -T33) has the widest lateral extent and comprises the subhorizontal sands and fine gravels that exhibit onlap relationships (T27, T28 and T29).

Based on these observations, a chronostratigraphic chart consisting of 34 timesteps is presented (Figure 16) which shows the distribution of the respective facies, the sedimentological events as time steps, and the stratal relationships of the facies, building the basis for chronostratigraphic interpretation described in chapter 4.

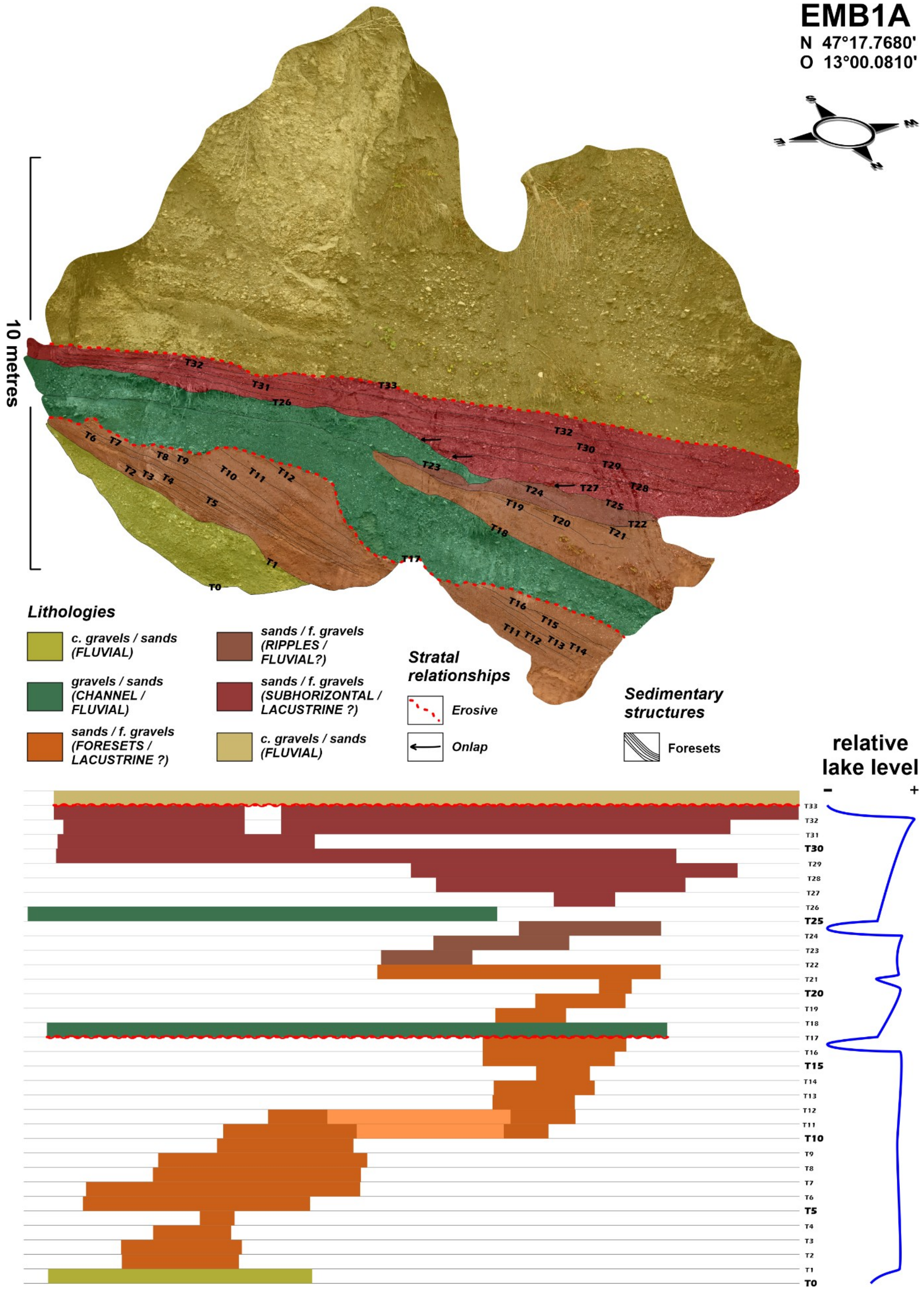

Figure 16: orthomosaic displaying different lithologies / facies; black lines represent timelines T0 – T33; chronostratigraphic chart on the bottom based on lateral extent of the timelines and stratal relationships of facies and respective relative lake level curve

3.5 Measurements

62 measurements of dip and dip direction of the features mentioned in chapter 2.1.2, were plotted as rose diagrams with corresponding great circles plotted in a stereographic net, 15 of them were derived digital and only plotted in a rose diagram. The rose diagrams are built as follows: the outermost circle represents the proportional share of the class with the highest frequency; the class size or interval has 10 ° steps. The general direction of the datasets is represented by the dashed black line, labelled with the respective value. For the directional analysis (rose diagrams) of the imbrications, the measured data need to be rotated by 180 ° as the structure dips against the flow direction.

3.5.1 Cross bedding

At outcrop EMB1A the general direction of the cross bedding is going towards North-North-West (NNW) with 340.80 ° (Figures 17A, 17B) and at outcrop EMB1B the mean direction is North-West (NW) with 312.00 ° (Figures 17C, 17D). The mean direction of all cross beddings combined is NNW at 338.10 ° (Figures 17E, 17F).

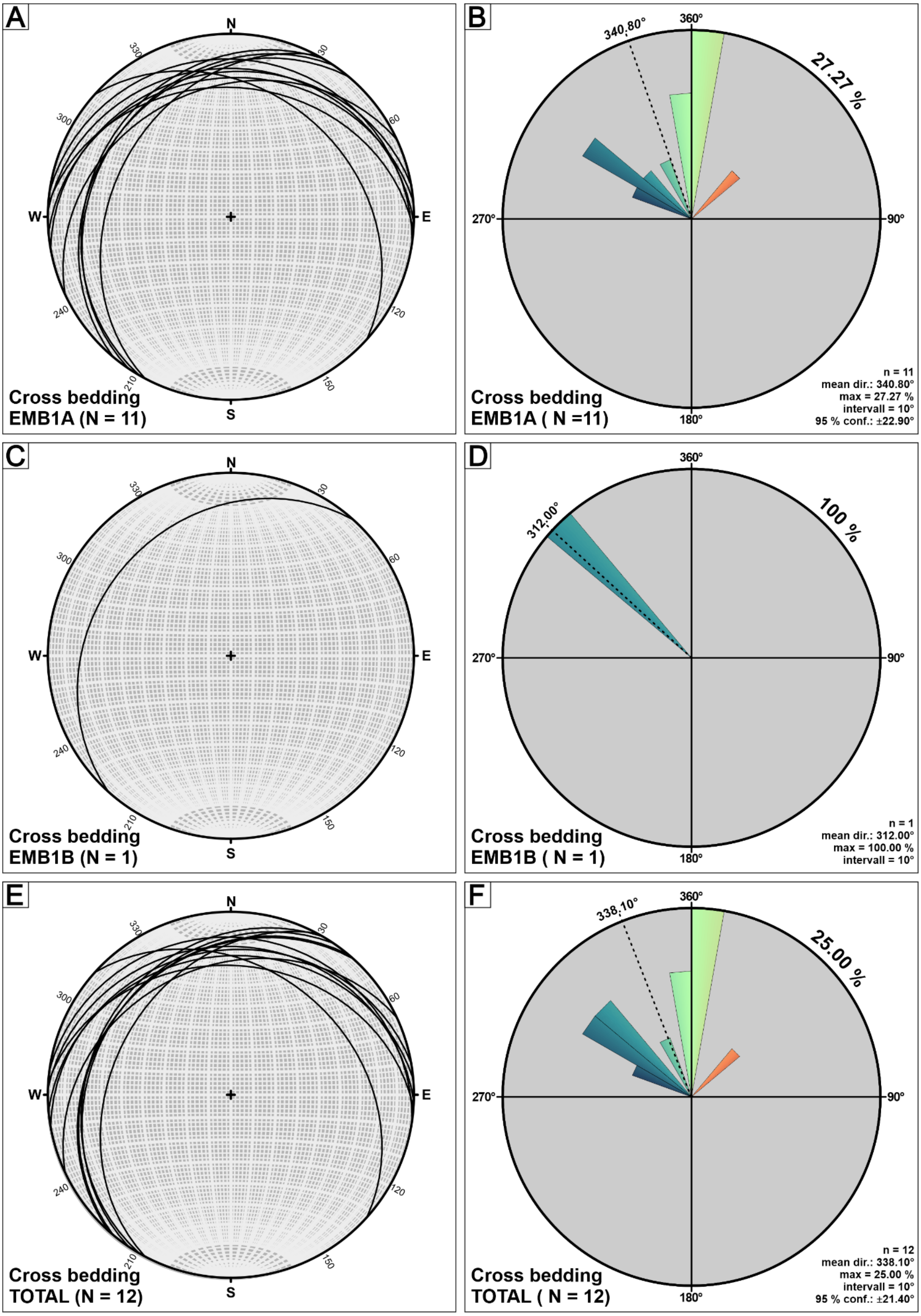

Figure 17: cross bedding of EMB1A, EMB1B and combined; general direction of cross bedding NNW

3.5.2 Imbrications

Gravel imbrication measured at EMB1A point towards North-East (NE) at an angle of 38.80 ° (Figures 18A, 18B), contrary to outcrop EMB1B, where the mean direction goes towards North-West-to-North (NWtN) with 324.00 ° (Figures 18C, 18D). The data of outcrop EMB3 (Figures 19A, 19B) are similar to EMB1A, although it is slightly more northerly at 24.60 ° (NNE). Considering the combined data of all imbrications (Figures 19C, 19D), the general direction goes towards NNE with an angle of 21.70 °.

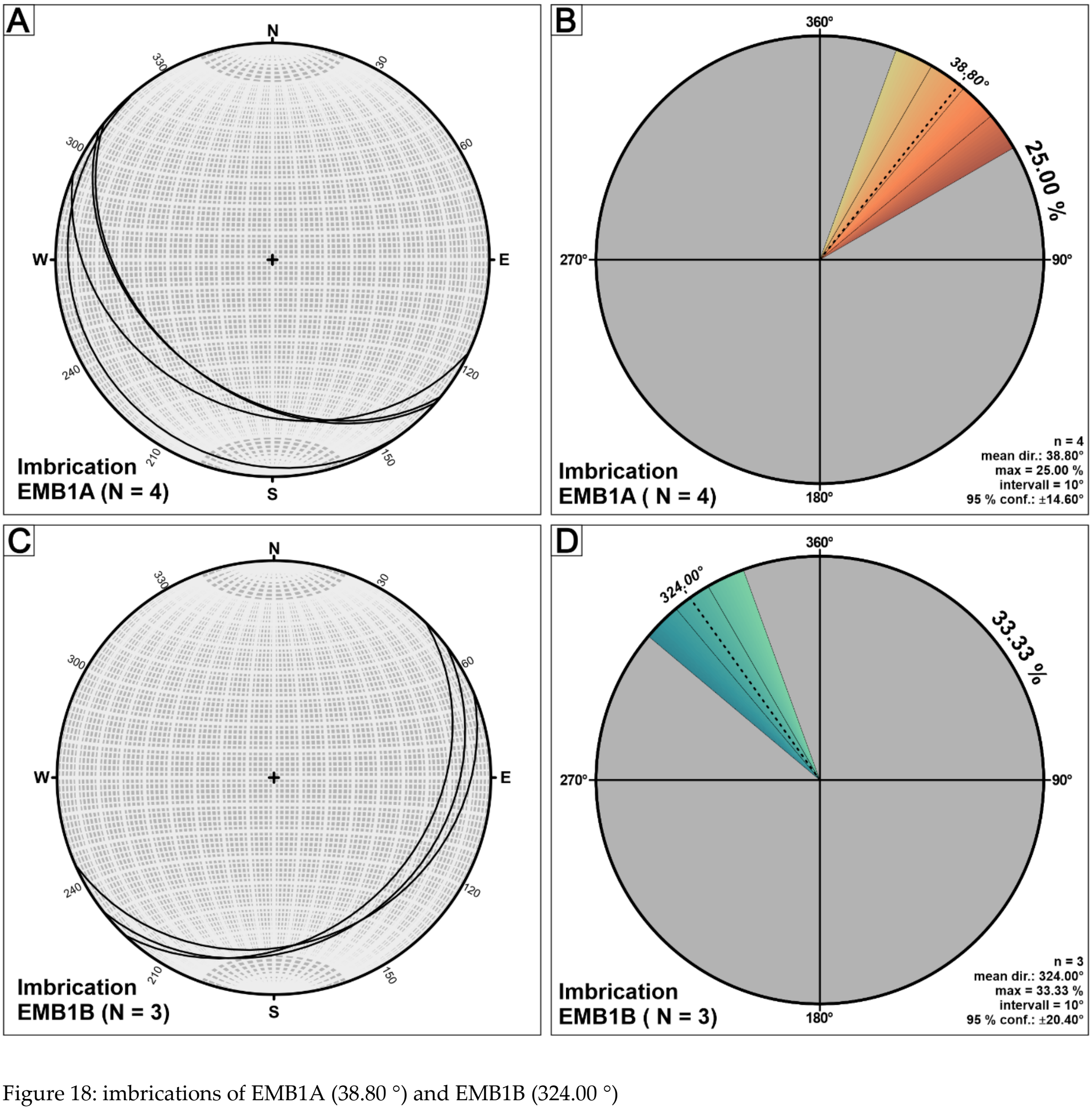

Figure 18: imbrications of EMB1A (38.80 °) and EMB1B (324.00 °)

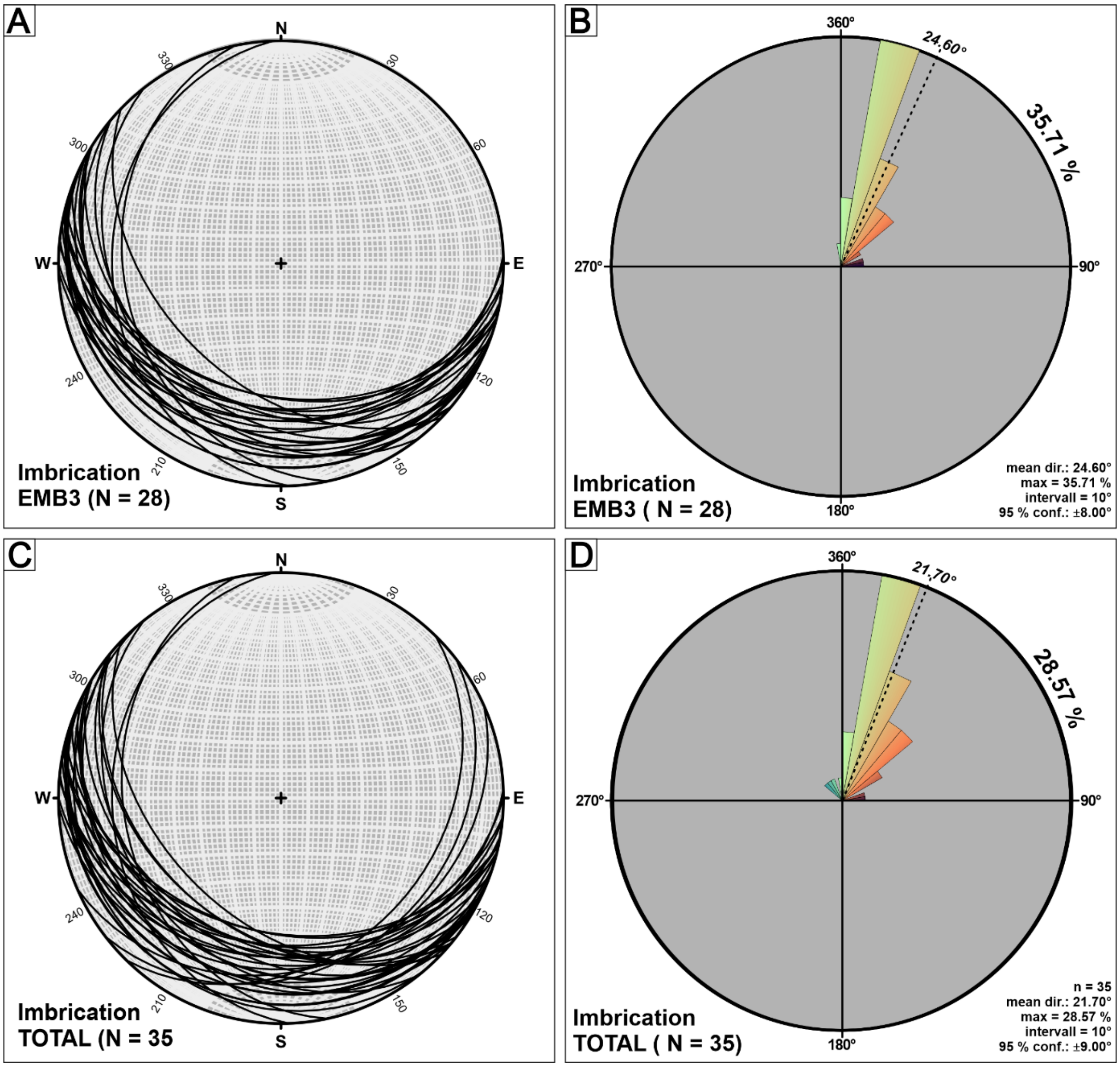

Figure 19: imbrications of EMB3 and all three outcrops combined, general flow direction going NNE (21.70 °)

3.6 Granulometry / sieving

The grain size distribution data received from dry- and wet-sieving, as well as from the Sedigraph analysis are displayed as grain size distribution curves (Figure 20) and a bar chart (Figure 21). Table 3 presents the obtained data in wt % at the end of this chapter.

Based on the curves, it can be seen that the sand and gravel samples (EMB1AS1-EMB3S2) are similar to each other but clearly differ from the till sample (EMB4BS2). Comparing the silt and clay contents reveals not only differences of the till to the sand and gravel samples, but also smaller differences of the sand and gravel samples among each other (Figure 21).

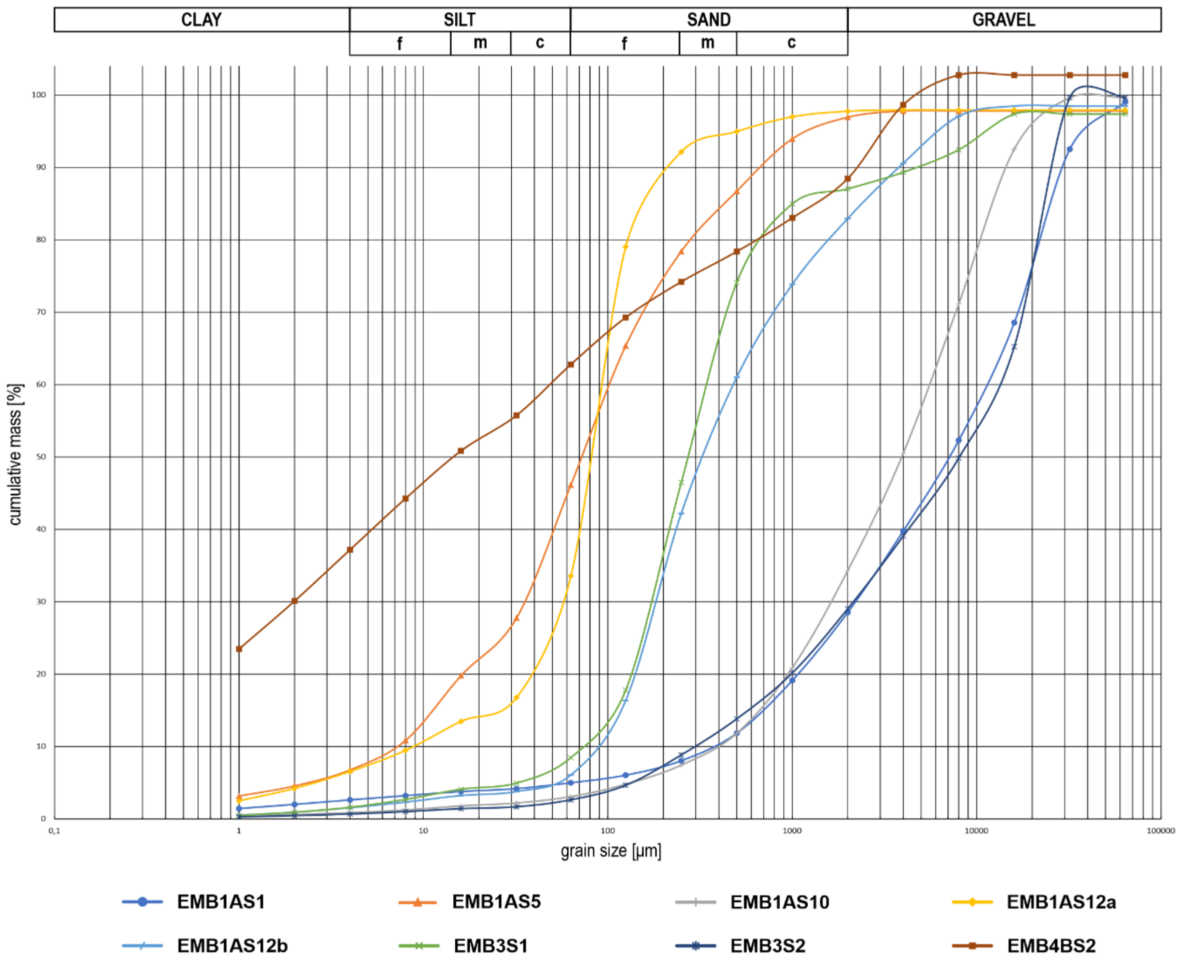

Figure 20: grain size distribution curves obtained from sieving and sedigraph analysis

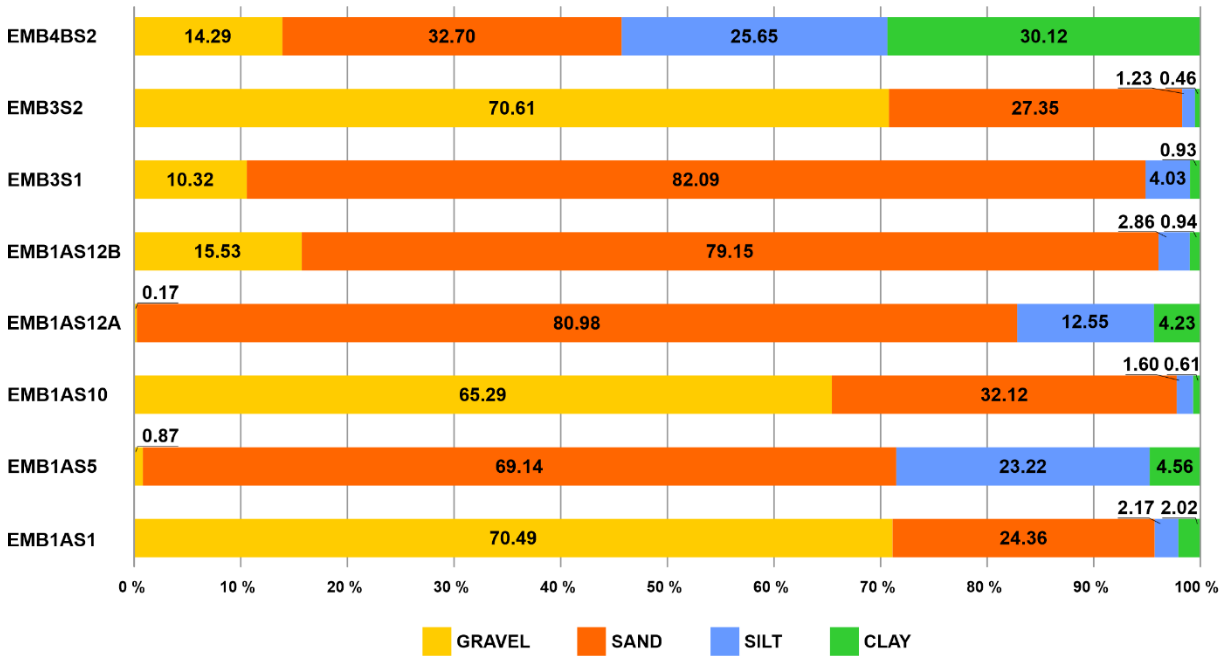

Figure 21: contents of grain sizes for each sample

The ternary diagram below shows the classification of the samples after Folk (1954), derived from GRADISTAT (Blott & Pye, 2001) and modified thereafter.

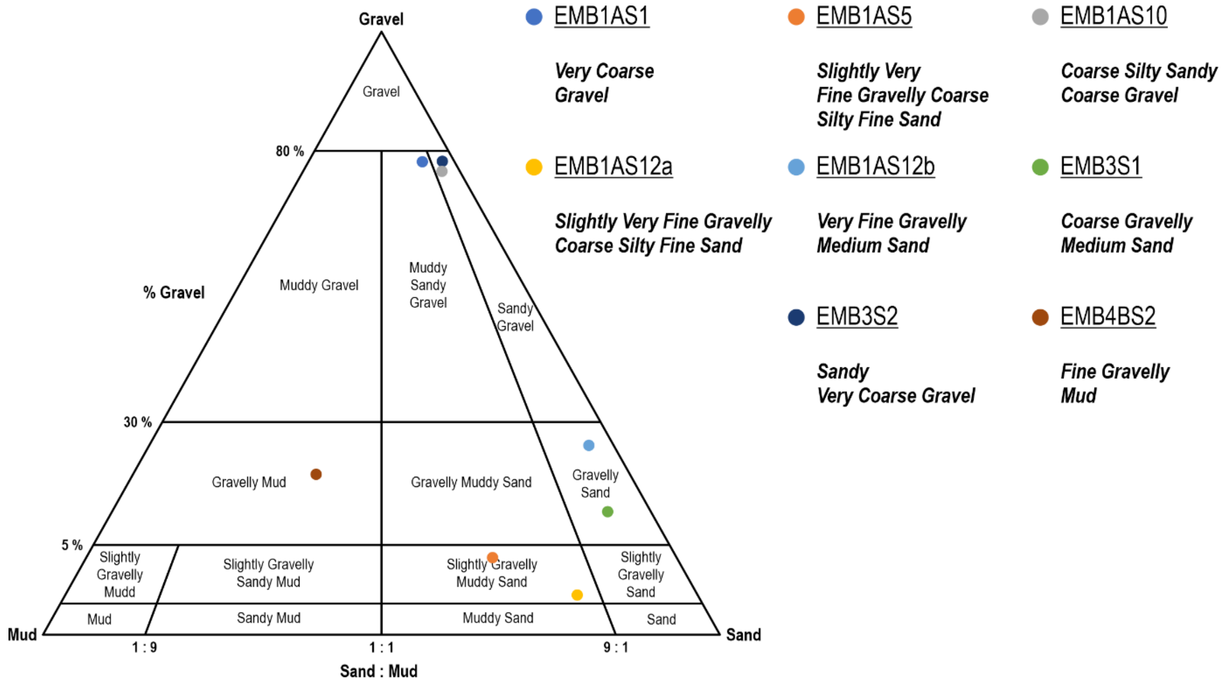

Figure 22: classification after Folk (1954); derived from Blott & Pye (2001) and modified thereof

Table 3: percentages of each grain size fraction obtained by sieving and sedigraph analysis

Grain size [mm]	EMB 1A S1 [wt %]	EMB 1A S5 [wt %]	EMB 1A S10 [wt %]	EMB 1A S12a [wt %]	EMB 1A S12b [wt %]	EMB 3 S1 [wt %]	EMB 3 S2 [wt %]	EMB 4B S2 [wt %]
> 64	6,52	0,00	0,00	0,00	0,00	0,00	0,00	0,00
> 32	23,95	0,00	7,08	0,00	0,00	0,00	34,40	0,00
> 16	16,25	0,00	21,36	0,00	1,40	4,92	15,38	0,00
> 8	12,53	0,00	20,66	0,00	6,49	3,11	10,78	4,11
> 4	11,24	0,87	16,19	0,17	7,64	2,29	10,05	10,18
> 2	9,41	2,98	13,45	0,77	9,10	2,08	8,87	5,44
> 1	7,30	7,22	9,05	2,03	12,83	10,86	6,34	4,65
> 0,5	3,80	8,33	4,39	2,82	18,82	27,64	4,98	4,18
> 0,25	1,99	13,03	2,65	13,10	25,82	28,67	4,19	4,93
> 0,125	1,05	19,22	1,71	45,47	10,29	9,32	2,01	6,48
> 0,063	0,81	18,36	0,87	16,79	2,29	3,52	0,96	7,02
> 0,032	0,40	7,97	0,41	3,29	0,56	0,85	0,26	4,91
> 0,016	0,57	8,95	0,56	4,01	0,90	1,41	0,41	6,58
> 0,008	0,59	4,08	0,38	2,92	0,78	1,09	0,33	7,08
> 0,004	0,61	2,22	0,25	2,33	0,62	0,68	0,23	7,08
> 0,002	0,58	1,39	0,20	1,73	0,42	0,45	0,18	6,64
< 0,002	1,44	3,17	0,41	2,50	0,52	0,48	0,28	23,48

3.7 Clast analysis

Concerning the clast roundness, both datasets, EMB1A and EMB4B, show a similar pattern (Figure 23) with subrounded clasts having the highest and subangular clasts having the second highest percentages. The only difference between both samples lies in the percentages of angular and rounded clasts. EMB1A has more angular than rounded clasts, EMB4B shows quite the opposite.

The measurements of the clasts axis lead to ternary plots (Figure 23) according to the method described in chapter 2.6, whereby both datasets show strong differences. Data points of EMB1A are distributed randomly over the plot with no cognisable clustering, whereas data points of EMB4B show a slight clustering below the C-40 line with only a few outliers.

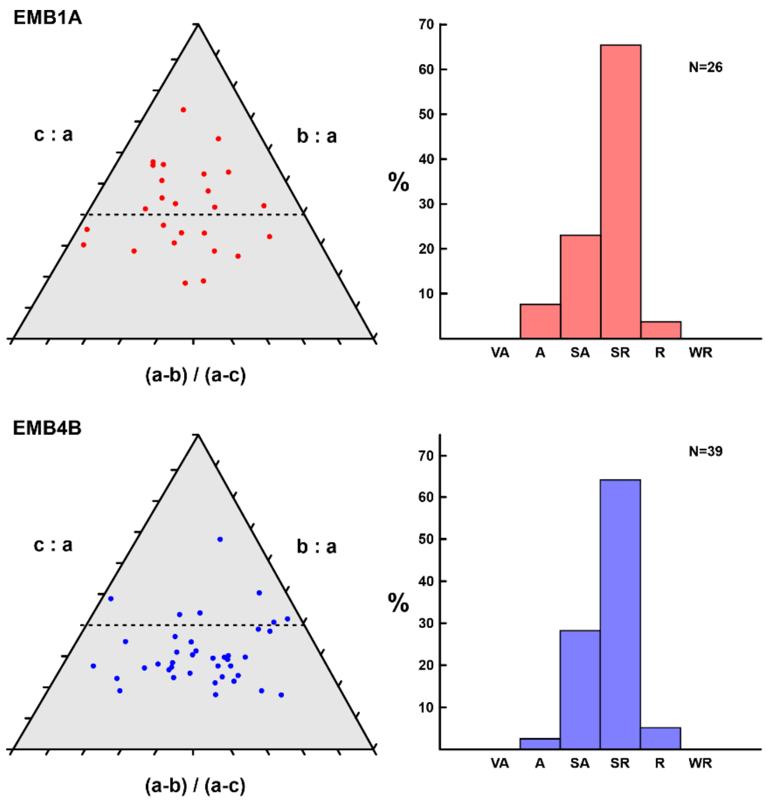

Figure 23: ternary diagrams of EMB1A and EMB4B after Graham & Midgley (2000); histograms displaying clast roundness of EMB1A and EMB4B

3.8 XRD

Figure 24 shows that the bulk mineral composition analysis via XRD of all samples show similar patterns and consist of Quartz, Calcite, Feldspars (Albite and Microcline), Muscovite, Chlorite, Paragonite and Amphibole.

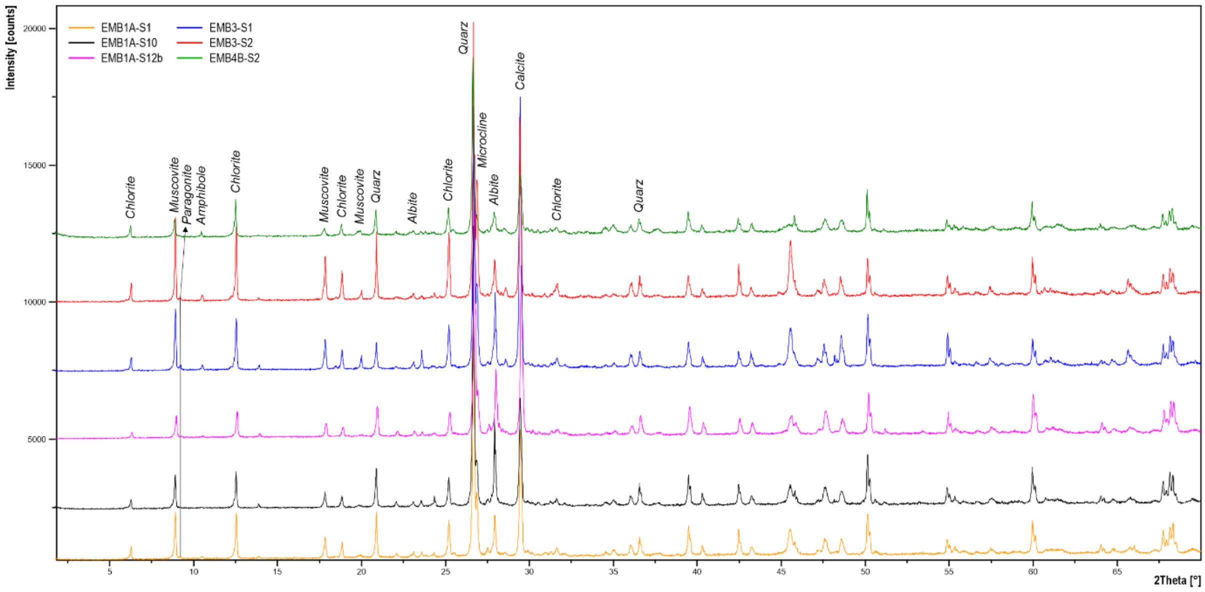

Figure 24: .X-ray diffraction patterns of the bulk samples

4 Interpretation

4.1 Basic sedimentological interpretations

4.1.1 Sediment source area

Clast analysis of samples EMB1AS1 and EMB4BS1 revealed three dominant lithologies (quartzite, mylonitic carbonate (Klammkalk) and phyllites) (Figures 11, 12). Sand, gravel and diamiction samples, described in chapters 2.1.3 and 3.2, consistently reveal similar XRD - patterns, interpreted to record the same mineralogical assemblage (Figure 24). Directional data gathered at the outcrops (chapter 3.5) confirms palaeoflow toward the north and northeast. This contrasts with the orientation with the orientation of drumlins (chapter 3.1.1) which record the eastward flow of the Salzach glacier.

Integrating lithological, mineralogical and palaeocurrent analysis, these datasets allow us to place constraints on sediment provenance. Hence, we interpret the sediments to have the same source area, represented by the Tauern Window immediately south and southwest to the section.

4.1.2 Sediment transportation

Based on the clast analysis, clast shape and surface texture respectively, two different modes of transportation can be interpreted, (i) fluvial transportation (EMB1A) and (ii) subglacial transport (EMB4B). Although the data of EMB4B did not reveal the expected result of the method described in chapter 2.6, we still interpret this sediment as subglacially transported, as most of these clasts are striated.

4.1.3 Depositional environment

Samples EMB1AS1, EMB1AS10 and EMB3S2 can be interpreted as fluvial sediments reflecting higher flow regimes than the other samples, as they have a high fraction of gravels (65.29 % - 70.61 %) and a relatively small fraction of silt or clay (~ 4 % maximum). In contrast, samples EMB1AS5, EMB1AS12A, EMB1AS12B and EMB3S1 had to be deposited at lower flow energies, as the major fraction is sand (79.15 % - 82.09 %) and they also tend to have higher percentages of silt and clay (~ 4-28 %). Sample EMB4BS2 is completely different to the others with 55.77 % of clay and silt, 32.70 % sand and 14.29 % gravel. Therefore, we interpreted this as subglacial deposit of a fine-grained matrix, bearing loose coarser clasts.

4.2 Facies interpretation

On basis of these lithologies and the geometries observed in the field and 3D model, a set of various facies was established, namely (1) a fluvial facies at the base of the section, (2) a deltaic/shallow lacustrine facies represented by N-dipping foresets, (3) a second fluvial facies which is laying discordant over (1) & (2) and can be interpreted as channel, (4) a second deltaic/lacustrine facies or another fluvial facies (consisting of either very poorly-developed foresets or large scale current ripples), (5) a (sub-)horizontal layered deeper lacustrine facies which is unconformably overlain by (6) a fluvial facies that is very similar to (1), (7) a third layer of deltaic / shallow lacustrine facies with finer sediments and much thinner crossbedding / foresets, (8) a horizontally layered, deeper lacustrine facies thin layer fine grained sediment and finally (9) a subglacial facies on top of the section.

These facies and their stratal relationships are emphasised in (i) Figure 25, displaying the whole sedimentary succession based on a simplistic sketch log and (ii) Figure 26 correlating the logs made in the field based on the facies elucidated above.

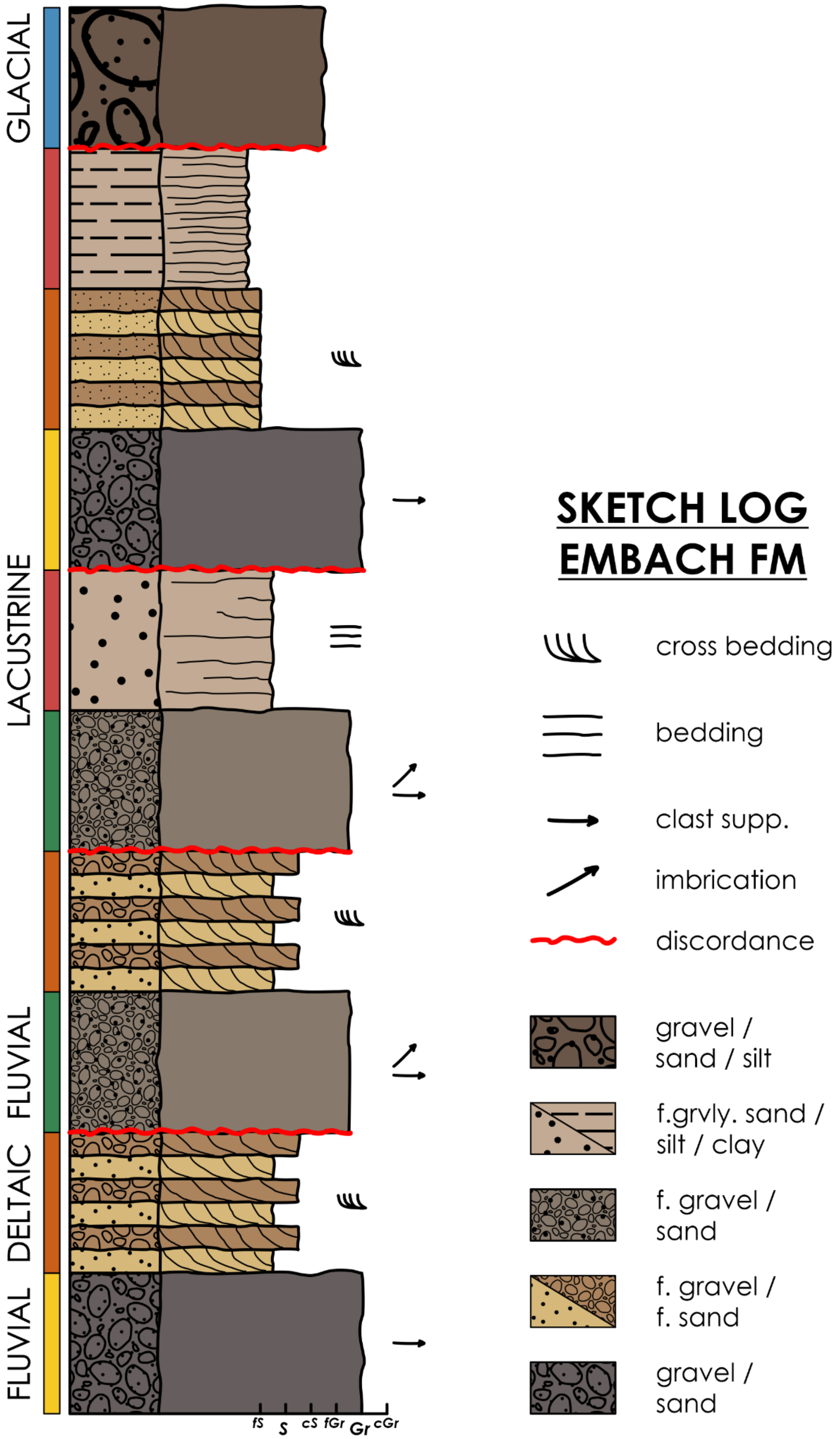

Figure 25: sketch log of the sedimentary succession at Embach

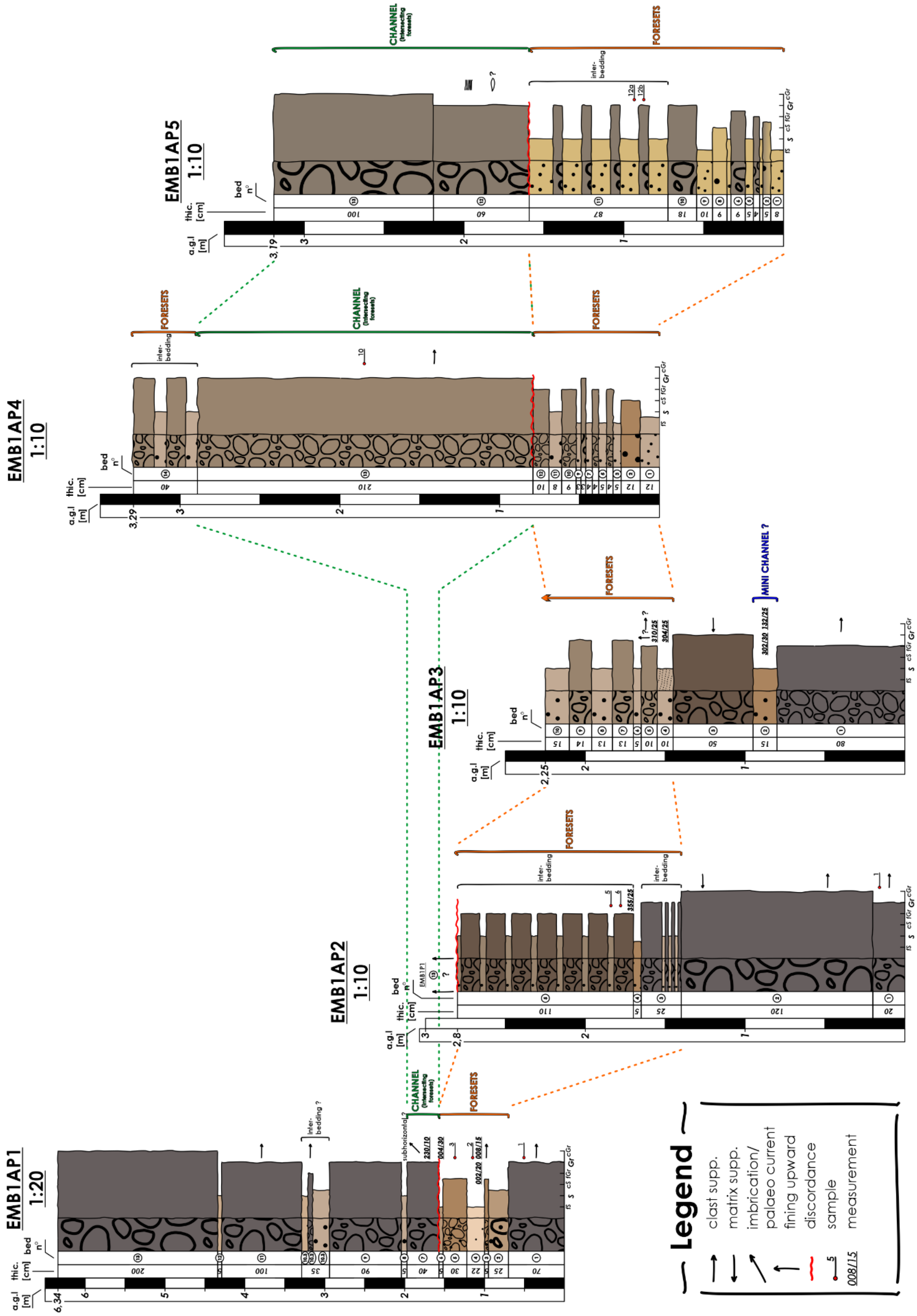

Figure 26: interpretation and correlation of detailed sedimentary logs

4.3 Paleoenvironmental reconstruction

The Embach succession represents a stable, gravelly ice-contact deltaic system whose sedimentary architecture probably reflects the dynamic interplay between glacial meltwater discharge, shifting sediment supply, and evolving accommodation space. Ice contact fans tend to evolve to ice-contact deltas (Dietrich et al., 2017; Lønne, 1995) and stable deltas tend to form in the lee of bedrock highs that can act as pinning points during glacial stillstand or retreat (Winsemann et al., 2007, 2011). The facies association records the transition from proximal delta-front gravels to more distal sandy foreset and bottomset deposits. The characteristics match those of a "clean river" homopycnal littoral delta (Zavala et al., 2021).

The scale of the foresets- reaching an amplitude of approximately 5 m - are compatible with a prograding delta slope and were probably generated by cohesionless debris flows (Sohn et al., 1997). The truncation of the foresets by irregular channel-like gravels has two plausible interpretations. The first is that these record abrupt base-level fall and incision of the delta slope, followed by the deposition of a fluvial topset characterised by either 3D dunes or gravelly sheet flows (Gruszka & Zieliński, 2021). The second possibility is that these represent chute and pool structures, produced by a cyclic step on the delta slope. In recent years, delta architecture has been recognized to include a range of cyclic step deposits which explains upslope-migrating dune bedforms in some deltas (Winsemann et al., 2018 and references therein). However, at Embach, the rather simple slope architecture and absence of backsets or climbing dunes (sensu Ghienne et al., 2010) favours a "traditional" interpretation of base-level fall, fluvial channel incision and fill. On the topsets, planar and trough cross-bedding record the migration of small- to medium-scale dunes and bars under strong unidirectional currents. In gravelly intervals, clast imbrication indicates a dominant palaeoflow toward the NE.

At the foreset to bottomset transition, climbing ripples and accretionary bedsets characteristic of such zones (c.f. Le Heron et al., 2023; Salamon & Zieliński, 2023) are missing. This lends further support to the idea that the foresets were built through grainflow avalanches rather than the supercritical flows so commonly recognised in other Pleistocene glacial deltas (e.g. Dietrich et al., 2017; Winsemann et al., 2018). Locally, matrix-supported gravels and poorly sorted intervals suggest sediment reworking by debris flow or hyperconcentrated flow pulses, reflecting brief episodes of enhanced sediment delivery or flow turbulence. Collectively, all these processes are consistent with deposition near a delta apex, where steep gradients and variable discharge promote short-lived but powerful sediment-laden flows. The alternation between clast-supported and matrix-supported gravels over a few decimetres implies fluctuations between streamflow-dominated and mass-flow-dominated conditions.

Considering the detailed profiles, EMB1P1 through EMB1P5 collectively represent the range of deltaic slope and subaerial topset deposits to more distal foreset and bottomset settings where sands dominate and beds tend to be thinner. The frequent erosional contacts described in several profiles suggest channel scour and subsequent infill, consistent with lateral shifting of distributary channels across the delta front. Local discordances between successive gravel-sand alternations may reflect minor avulsion or reoccupation of flow paths. The well-expressed subhorizontal planar bedding across the Embach outcrop, likely developed in low-relief topset areas where tractional sheet flows spread across the delta plain (Gruszka & Zieliński, 2021).

During the LGM, the Salzach glacier flowed from west to east (Figures 3, 4) over Embach depositing diamicton which was locally drumlinised in the subglacial environment. The overconsolidated composition of the diamicton, together with the abundance of striated clasts that it contains, together represent classic indicators of a till consistent with the geomorphological mapping interpretations. Overconsolidation develops during a combination of dewatering, shear and ploughing which lead to the characteristic hardened texture of Pleistocene subglacial tills (Clarke, 2018).

5 Discussion

5.1 Damming mechanism and relative lake level fluctuation

The results and the interpretations derived from them, unequivocally prove the existence of a pre LGM lake at the site of Embach. This premises that (i) the Salzach valley was already partly formed influenced by earlier glaciations (Günz, Mindel and Riss) and (ii) due to the relief of the Salzach Valley, a damming mechanism east of Embach is crucial, interrupting water discharge of the area and therefore building up the lake. Numerous hypotheses could be put forward explaining the damming including (i) collapse of hanging glaciers from one of the lateral valleys, (ii) glaciers from lateral valleys, (iii) collapse of lateral moraines of the Salzach glacier or terminal moraines from glaciers of lateral valleys, (iv) alluvial fans of tributaries draining to the north or south into the Salzach Valley and bearing loads of sediment, and (v) slope failure or mass movement (Figure 27).

Moraine dammed lakes are common in the Alps (Buckel et al., 2018; Griesmeier et al., 2025). Likewise, the generation of alluvial fans has also been proposed as a damming mechanism prior to the LGM in Ennstal (Le Heron et al., 2023). Dietrich (1990) and references therein showed that mass movement in the area of Embach already occurred during the Quaternary between Riss and Würm glaciations respectively. Hypotheses involving ice as damming mechanism are considered less likely, as the sedimentary succession was deposited between the Riss and Würm glacial cycles, and thick, valley-filling trunk glaciers would not have been present. Each of these possible mechanisms would have had the same results: cutting off the drainage of the Salzach river and damming it to form a lake. Given the unlikelihood of a glacier damming mechanism on stratigraphic grounds, it is proposed that moraine collapse, general slope failure / mass movement, or alluvial fan development are all plausible mechanisms. Based on current data, it is not possible to identify which is most likely; rather, this is a topic for future research.

The relative lake level curve (Figure 16) takes the interpreted mechanism of lake initiation into account. Assuming that the damming mechanism was provided by a landslide, rock fall, moraine collapse, or rapid depositional event on an alluvial fan, a 3-stage sequence of possible events could be proposed. First, the mass movement would dam the Salzach river leading to a rise in lake level and transgression. Second, partial collapse or slow erosion of the dam would lead to gradual reduction in lake level or regression. Thirdly, a subsequent slope failure / mass movement into the lake would provide the mechanism for a renewed transgression (Figure 27). Dietrich (1990) and references therein mentioned early documented events (16th and also 18th century), where this was the very reason for damming Salzach river, leading to flooded infrastructure.

Looking at the literature, there are thus historical precedents for the "collapsed-moraine-hypothesis", the "slope-failure-hypothesis" and the "alluvial-fan-hypothesis": the course of events regarding the dam breaching or dam erosion *per se* would remain the same, the difference would lie only in the sediment source.

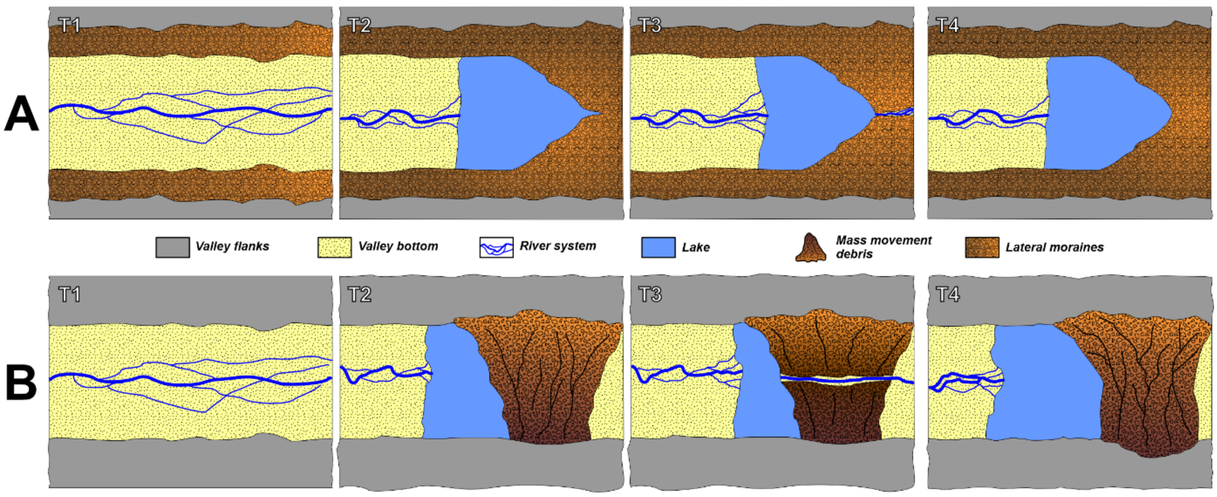

Figure 27: (A) sketch of lateral-moraine-damming-hypothesis and (B) sketch of mass movement-damming-hypothesis; both divided in four timesteps (T1-T4) demonstrating (i) damming and (ii) relative lake level fluctuations

As in many Quaternary studies, an important unknown element remains: the time frame over which sediment was deposited. It was out of scope of this project, with a strong focus on outcrop sedimentology and granulometry, to undertake optically stimulated luminescence (OSL) dating, yet this has proven to be important for geochronology of similar glaciofluvial and deltaic deposits in Ennstal (Griesmeier et al., 2025). Subsequently, the sequence stratigraphic approach must account for both episodic events (rockfalls and moraine collapse as damming mechanisms), sufficient time to generate discordances, and diachroneity in delta development. To the author's knowledge, no study specifically focussing on diachroneity has been attempted in deltaic deposits of the *Vorstoßschotter* deposits but useful insights can be gained from larger delta systems. For example, Wang et al. (2025) examined the lag time between sediment supply and delta response: increasing supply of river sediment has a lag time of 1 year, decreasing sediment supply resulted in a lag time (response) of 6 years.

5.2 Wider significance of the Embach section

Together with some recently described sections in Enns Valley (Griesmeier et al., 2025; Le Heron et al., 2023), the Embach section is one of a limited number of outcrops now recognised to reflect the development of a pre-LGM delta system. The logical implication of this is that we can propose the existence of a pre-LGM lake for the first time in the Salzach Valley. Consequently, this interpretation raises the possibility that previous interpretations that the *Vorstoßschotter* are fluvial deposits (Reitner, 2022; Van Husen, 1983), should be re-evaluated. The distinction between fluvial and deltaic systems is important, and suggests that the depositional setting of the *Vorstoßschotter* is likely more complex than previously thought, with elements of fluvial and deltaic sedimentation. A systematic reinvestigation of such deposits may reveal that delta deposits are more widespread than previously thought.

Brandner (2017) and Dietrich (1990) found a thin layer of lacustrine clay sandwiched between the sand and gravels below and the till above. In the present study no such clay deposit was encountered during fieldwork in 2024 and 2025, and is attributed to either progressive erosion of the outcrop or growth of vegetation. Nevertheless, this observation provides further evidence substantiating the existence of a lake system. Furthermore, in the eastern part of Embacher Plaike, a section of finer grained but inaccessible sediment (vertical slope) could be recognised on UAV imagery (intervals highlighted in yellow and red on Figure 9D). As the lower interval (yellow) shows structures resembling cross stratification, an interpretation as clay is unlikely. This leaves only the upper interval (red), a few cm to dm thick layer with no structures observed, remaining which could be interpreted as clay.

5.3 Data limitations

5.3.1 Palaeo flow direction vs source area

Figure 28 illustrates that palaeoflow directions inferred from foresets and imbrications in the fluvial-deltaic sediments do not align perfectly with drumlin orientations. This discrepancy might suggest that the underlying sands-gravels and capping till were derived from distinct source areas.

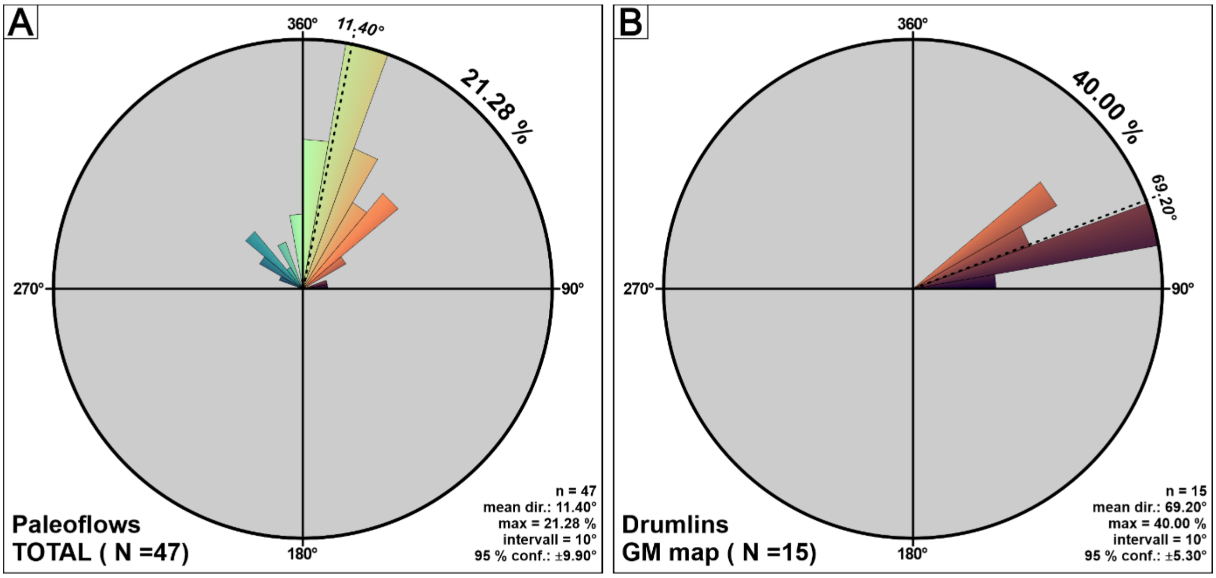

Figure 28: comparison of flow directions of foresets & imbrications (A) and flow directions of glacial movement (B)

This interpretation can be countered by considering the ice-flow dynamics: the till-forming ice likely advanced from a more southerly source, such as the Rauris Valley, before merging with the dominant west-to-east Salzach trunk glacier at the valley confluence. This merger would have deflected the Rauris ice stream eastward, aligning its sediment delivery with the observed drumlin field. Moreover, the Tauern Window extends far west and southwest of the study area, ensuring a broadly shared regional provenance even if the till reflects input from lateral tributaries; subglacial entrainment by the Salzach Glacier could then transport this material to Embach.

A counterargument arises from the clast lithologies, which - despite overlap - vary in relative abundance between outcrops (e.g., Klammkalk dominance in EMB4B vs gneiss-quartzite in EMB1A). Such differences question whether the till and pre-LGM sediments truly share an identical source.

5.3.2 Granulometry / Sieving

Irregularities in the cumulative grain-size curves likely stem from methodological limitations, including inconsistencies in sample preparation and sieving, as well as variable precision between dry sieving (>2 mm), wet sieving (0.063–2 mm) and Sedigraph analysis (<0.063 mm).

5.3.1 Clast analysis

As outlined in Section 2.6, the C40 line demarcates active transport domains (e.g. subglacial; upper field) from passive ones (e.g. supraglacial/englacial; lower field) following Graham & Midgley (2000). Subglacial tills typically cluster above this threshold, yet EMB4B data plot predominantly below it. The deposit is nevertheless interpreted as till based on its overconsolidated fabric, matrix-supported texture and abundant striated clasts.

5.4 Further research / remaining uncertainties

Additional work is essential to clarify pre-LGM landscape evolution across Austria, particularly the *Vorstoßschotter* and analogous units. Confirming damming mechanisms - for example via targeted coring or geophysical profiling - would refine the palaeoenvironmental model and inform geohazard mitigation at Embach. Provenance studies, including U-Pb geochronology of detrital zircons, could resolve whether till and delta-fluvial sediments share a common source, while quantifying interglacial sediment fluxes would contextualise depositional rates.

Ongoing erosion and mass wasting necessitate integrated geomechanical analyses linking sedimentary architecture to slope instability. Combining geophysical surveys (e.g., GPR, ERT) with subsurface imaging would delineate sediment-bedrock transitions, optimising stabilisation strategies such as enhanced drainage or buttressing.

6 Conclusions

Detailed investigation of the Quaternary succession in Embach, Salzburg, allows four key conclusions to be drawn, casting new light into the development of this area prior to and during the LGM:

- **Delta-fluvial sedimentation in a dammed valley**: The ~80 m thick sands and gravels record repeated cycles of lake-level rise and fall within a partly lake-filled Salzach Valley, as evidenced by sequence-stratigraphic analysis of 33 discrete sedimentary events across five facies (coarse gravel-sand, cross-stratified sands-fine gravels, subhorizontal sands). Large-scale foresets (up to 5 m amplitude) document prograding gravelly delta fronts fed by north- and east-directed palaeoflow, while imbricated channel fills and sheet gravels reflect fluvial incision during base-level falls, overturning prior interpretations of *Deckenschotter* as purely fluvial;
- **Damming mechanisms and lake dynamics**: Episodic lake formation likely resulted from various processes, including collapse of hanging glaciers or lateral moraines from tributary valleys (Gasteiner and Rauriser), mass movements along the steep valley flanks, or progradation of alluvial fans from northward- or southward-draining rivulets, as inferred from stratal onlap relationships (e.g., T27–T29) and the topographic context of overdeepened bedrock basins formed during pre-LGM glaciations;
- **Sediment provenance and transport pathways**: Clast lithologies (gneiss, quartzite, mylonitic carbonate, phyllite) and XRD mineralogy (quartz, calcite, feldspars, muscovite) match the northeastern Tauern Window, with fluvial transport dominant in sands and gravels (randomly distributed c/a ratios, subrounded shapes) versus subglacial transport in the capping overconsolidated till (clustered below C40 line, striated clasts), confirming a shared proximal source upslope of the study area;

- **Regional glacial context and LGM overprint**: Drumlin orientations (ENE, 69.2 °) and subglacial channels align with west-east Salzach glacier flow, which deposited the basal till during LGM advance; palaeocurrent contrasts (NNW foresets, NNE imbrications) highlight pre-LGM axial infill by tributary systems, paralleling lake-delta records in the eastern Enns Valley and suggesting widespread undocumented impoundments across Alpine trough valleys.

  In addition, the study has highlighted promising avenues for further research including the prospect of finding further deltaic successions in the Deckenschotter deposits elsewhere in Alpine terrain, and the hunt for damming mechanisms to understand the development of intramontane lakes.

References

Allmendinger, R. (2024). *Stereonet* (Version 11) [Software]. https://www.rickallmendinger.net/stereonet

Benn, D. I., & Ballantyne, C. K. (1994). Reconstructing the transport history of glacigenic sediments: A new approach based on the co-variance of clast form indices. *Sedimentary Geology*, *91*(1–4), 215–227. https://doi.org/10.1016/0037-0738(94)90130-9

BEV, (2022). *Topographische Karte des Bundeseich- und Vermessungsamts* [Map]. https://maps.bev.gv.at/#/center/13.35,47.7702/zoom/8

Blott, S. J., & Pye, K. (2001). GRADISTAT: A grain size distribution and statistics package for the analysis of unconsolidated sediments. *Earth Surface Processes and Landforms*, *26*(11), 1237–1248. https://doi.org/10.1002/esp.261

Boggs, S. (2006). *Principles of sedimentology and stratigraphy* (4. ed). Pearson Prentice Hall.

Brandner, K. (2017). Konzeptionelles hydrogeologisches Modell rezenter Massenbewegungen am Beispiel der Embacher Plaike und Hochebene, Salzburg, Österreich. *Beiträge zur Hydrogeologie*, *61*, 61–72.

Buckel, J., Otto, J. C., Prasicek, G., & Keuschnig, M. (2018). Glacial lakes in Austria—Distribution and formation since the Little Ice Age. *Global and Planetary Change*, *164*, 39–51. https://doi.org/10.1016/j.gloplacha.2018.03.003

Clarke, B. G. (2018). The engineering properties of glacial tills. *Geotechnical Research*, *5*(4), 262–277. https://doi.org/10.1680/jgere.18.00020

Dietrich, M. (1990). *Geologische Untersuchungen der Hangbewegungen im Bereich der Taxenbacher Enge (Land Salzburg)*. TU München.

Dietrich, P., Ghienne, J., Schuster, M., Lajeunesse, P., Nutz, A., Deschamps, R., Roquin, C., & Duringer, P. (2017). From outwash to coastal systems in the Portneuf–Forestville deltaic complex (Québec North Shore): Anatomy of a forced regressive deglacial sequence. *Sedimentology*, *64*(4), 1044–1078. https://doi.org/10.1111/sed.12340

Emery, D., & Bertram, G. T. (1996). *Sequence Stratigraphy* (1. Aufl.). Blackwell Science.

Folk, R. L. (1954). The Distinction between Grain Size and Mineral Composition in Sedimentary-Rock Nomenclature. *The Journal of Geology*, *62*(4), 344–359. https://doi.org/10.1086/626171

Frost, E., Dolan, J., Sammis, C., Hacker, B., Cole, J., & Ratschbacher, L. (2009). Progressive strain localization in a major strike-slip fault exhumed from midseismogenic depths: Structural observations from the Salzach-Ennstal-Mariazell-Puchberg fault system, Austria. *Journal of Geophysical Research: Solid Earth*, *114*(B4), 2008JB005763. https://doi.org/10.1029/2008JB005763

Ghienne, J.-F., Girard, F., Moreau, J., & Rubino, J.-L. (2010). Late Ordovician climbing-dune cross-stratification: A signature of outburst floods in proglacial outwash environments? *Sedimentology*. https://doi.org/10.1111/j.1365-3091.2009.01142.x

Google Earth (Version 7.3.6.10441). (2025). [Software]. Google. https://earth.google.com

Graham, D. J., & Midgley, N. G. (2000). *Graphical representation of particle shape using triangular diagrams: An Excel spreadsheet method*.

Griesmeier, G. E. U., Le Heron, D. P., Lüthgens, C., Firla, G., Salcher, B., Dremel, F., Otto, J., & Reitner, J. M. (2025). Middle to Late Pleistocene landscape evolution and glacial dynamics in the Eastern Alps: The Gröbminger Mitterberg record, Austria. *Boreas*, bor.70045. https://doi.org/10.1111/bor.70045

Grohmann, C. H. (2025). *Openstereo* (Version 0.1.2) [Software]. Universidade de Sao Paulo. https://spamlab.github.io/pages/grants/openstereo/

Groß, P., Handy, M. R., John, T., Pestal, G., & Pleuger, J. (2020). Crustal-Scale Sheath Folding at HP Conditions in an Exhumed Alpine Subduction Zone (Tauern Window, Eastern Alps). *Tectonics*, *39*(2), e2019TC005942. https://doi.org/10.1029/2019TC005942

Gruszka, B., & Zieliński, T. (2021). Lacustrine deltas and subaqueous fans: Almost the same, but different – a review. *Geologos*, *27*(1), 43–55. https://doi.org/10.2478/logos-2021-0004

Ivy-Ochs, S., Kerschner, H., Reuther, A., Preusser, F., Heine, K., Maisch, M., Kubik, P. W., & Schlüchter, C. (2008). Chronology of the last glacial cycle in the European Alps. *Journal of Quaternary Science*, *23*(6–7), 559–573. https://doi.org/10.1002/jqs.1202

Kreuss, O. (2013). *Geofast—Zusammenstellung ausgewählter Archivunterlagen der Geologischen Bundesanstalt 1: 50000* (2018/05 Aufl.) [Map]. Geologische Bundesanstalt. https://www.tethys.at/dataset/133

Land Salzburg. (2017). *Laserscans (1 m)* [Software]. Land Salzburg. https://www.salzburg.gv.at/sagismobile/sagisonline

Le Heron, D. P., Griesmeier, G. E. U., & Reitner, J. M. (2023). A window into development of a complex ice-marginal lake prior to the Late Glacial Maximum (LGM) in Austria. *Geology*, *51*(10), 914–918. https://doi.org/10.1130/G51298.1

Lønne, I. (1995). Sedimentary facies and depositional architecture of ice-contact glaciomarine systems. *Sedimentary Geology*, *98*(1–4), 13–43. https://doi.org/10.1016/0037-0738(95)00025-4

Lukas, S., Benn, D. I., Boston, C. M., Brook, M., Coray, S., Evans, D. J. A., Graf, A., Kellerer-Pirklbauer, A., Kirkbride, M. P., Krabbendam, M., Lovell, H., Machiedo, M., Mills, S. C., Nye, K., Reinardy, B. T. I., Ross, F. H., & Signer, M. (2013). Clast shape analysis and clast transport paths in glacial environments: A critical review of methods and the role of lithology. *Earth-Science Reviews*, *121*, 96–116. https://doi.org/10.1016/j.earscirev.2013.02.005

Metashape (Version 2.1.3). (2024). [Software]. Agisoft. https://www.agisoftmetashape.com/

Perkins, D. (2025, September 22). Opengeology. *12 X-Ray Diffraction and Mineral Analysis*. https://opengeology.org/Mineralogy/12-x-ray-diffraction-and-mineral-analysis/

Reitner, J. M. (2022). The Imprint of Quaternary Processes on the Austrian Landscape. In C. Embleton-Hamann (Hrsg.), *Landscapes and Landforms of*

Austria (S. 47–72). Springer International Publishing. https://doi.org/10.1007/978-3-030-92815-5_3

Salamon, T., & Zieliński, T. (2023). Development of a Gilbert-type delta in the kame environment: An example from NE Poland. *Sedimentary Geology*, *455*, 106484. https://doi.org/10.1016/j.sedgeo.2023.106484

Salcher, B. C., Starnberger, R., & Götz, J. (2015). The last and penultimate glaciation in the North Alpine Foreland: New stratigraphical and chronological data from the Salzach glacier. *Quaternary International*, *388*, 218–231. https://doi.org/10.1016/j.quaint.2015.09.076

Salcher, B., Starnberger, R., Pollhammer, T., & Götz, J. (2024). Sediment dynamics of a major piedmont glacier: The Salzach Glacier in the North Alpine Foreland. *DEUQUA Special Publications*, *5*, 31–39. https://doi.org/10.5194/deuquasp-5-31-2024

Schmid, S. M., Scharf, A., Handy, M. R., & Rosenberg, C. L. (2013). The Tauern Window (Eastern Alps, Austria): A new tectonic map, with cross-sections and a tectonometamorphic synthesis. *Swiss Journal of Geosciences*, *106*(1), 1–32. https://doi.org/10.1007/s00015-013-0123-y

Schroll, M. (1798). Beschreibung des merkwürdigen Erfalls zu Embach im Pfleggerichte Taxenbach im Salzburgischen. *Jahrbücher der Berg- und Hüttenkunde*, *2*, 234–248.

Sedigraph III Plus. ((n.d.)). *GAT Scientific*. https://gatscientific.com/product/sedigraph-iii-plus/

Sneed, E. D., & Folk, R. L. (1958). Pebbles in the Lower Colorado River, Texas a Study in Particle Morphogenesis. *The Journal of Geology*, *66*(2), 114–150. https://doi.org/10.1086/626490

Sohn, Y.-K., Kim, S.-B., Hwang, I., Bahk, J., Choe, M., & Chough, S.-K. (1997). Characteristics and Depositional Processes of Large-scale Gravelly Gilbert-Type Foresets in the Miocene Doumsan Fan Delta, Pohang Basin, SE Korea. *Journal of Sedimentary Research*, *Vol. 67*, 130–141. https://doi.org/10.1306/D4268513-2B26-11D7-8648000102C1865D

Van Husen, D. (1983). A model of valley bottom sedimentation during climatic changes in a humid alpine environment. In *Tills and Related Deposits: Genesis, Petrology, Application, Stratigraphy* (S. 345–349). A. A. Balkema.

Van Husen, D. (2000). Geological Processes during the Quaternary. *Mitteilungen der Österreichischen Geologischen Gesellschaft*, *92*, 135–156.

Wang, J., Dai, Z., Mei, X., Duan, H.-F., & Nienhuis, J. H. (2025). Response time of global deltas to changes in fluvial sediment supply. *Nature Communications*, *16*(1), 5573. https://doi.org/10.1038/s41467-025-60531-9

Winsemann, J., Asprion, U., Meyer, T., & Schramm, C. (2007). Facies characteristics of Middle Pleistocene (Saalian) ice-margin subaqueous fan and delta deposits, glacial Lake Leine, NW Germany. *Sedimentary Geology*, *193*(1–4), 105–129. https://doi.org/10.1016/j.sedgeo.2005.11.027

Winsemann, J., Brandes, C., & Polom, U. (2011). Response of a proglacial delta to rapid high-amplitude lake-level change: An integration of outcrop data and high-resolution shear wave seismics: Response of a proglacial delta to rapid high-amplitude lake level change. *Basin Research*, *23*(1), 22–52. https://doi.org/10.1111/j.1365-2117.2010.00465.x

Winsemann, J., Lang, J., Polom, U., Loewer, M., Igel, J., Pollok, L., & Brandes, C. (2018). Ice-marginal forced regressive deltas in glacial lake basins: Geomorphology, facies variability and large-scale depositional architecture. *Boreas*, *47*(4), 973–1002. https://doi.org/10.1111/bor.12317

Zavala, C., Arcuri, M., Di Meglio, M., Zorzano, A., Otharán, G., Irastorza, A., & Torresi, A. (2021). Deltas: A new classification expanding Bates's concepts. *Journal of Palaeogeography*, *10*(1), 23. https://doi.org/10.1186/s42501-021-00098-w

Table of figures

Table of tables

Data availability

All primary data is available upon request to lukas.eder@univie.ac.at.